Energy Research and Development Division
FINAL PROJECT REPORT

ASSESSING THE ROLE OF WINTER FLOODING ON BASELINE GREENHOUSE GAS FLUXES FROM CORN FIELDS IN THE SACRAMENTO – SAN JOAQUIN BAY DELTA

Prepared for: California Energy Commission
Prepared by: The U.S. Geological Survey

SEPTEMBER 2013
CEC-500-2014-077

PREPARED BY:

Primary Author(s):
Brian Pellerin
Frank Anderson
Brian Bergamaschi

U.S. Geological Survey, California Water Science Center
6000 J Street, Placer Hall
Sacramento, CA 95819
bpeller@usgs.gov

Contract Number: 500-09-012

Prepared for:

California Energy Commission

Joe O'Hagan
Contract Manager

Joe O'Hagan
Project Manager

Aleecia Gutierrez
Office Manager
Energy Generation Research Office

Laurie ten Hope
Deputy Director
ENERGY RESEARCH AND DEVELOPMENT DIVISION

Robert P. Oglesby
Executive Director

DISCLAIMER

This report was prepared as the result of work sponsored by the California Energy Commission. It does not necessarily represent the views of the Energy Commission, its employees or the State of California. The Energy Commission, the State of California, its employees, contractors and subcontractors make no warranty, express or implied, and assume no legal liability for the information in this report; nor does any party represent that the uses of this information will not infringe upon privately owned rights. This report has not been approved or disapproved by the California Energy Commission nor has the California Energy Commission passed upon the accuracy or adequacy of the information in this report.

ACKNOWLEDGEMENTS

The U.S. Geological Survey thanks the California Energy Commission (particularly Joe O'Hagan and Sarah Pattiglio) for grant support to conduct this research as well as support from the USGS Federal Matching Funds program. The authors thankThe Nature Conservancy (Leo Winternitz, Sara Sweet and Greg Golet) and Brent Tadman of Conservation Farms and Ranches for site access and logistical support. The authors thank Katie Bednar, Kathleen Keating, and Paul Kreun at the USGS for field and lab support. The authors also thank Will Horwath, Yascov Assa, Jennifer Morris, Rhongzhong Ye, Martin Burger, and Tad Doane at UC-Davis for analytical support; Joe Verfaillie, Cove Sturtevant, Sara Knox, Laurie Koteen, and Dennis Baldocchi at UC-Berkeley for technical support; Justin Black, Todd Perceval, Kim Rosmaier, and Jason Harbaugh at the California Department of Water Resources for field and technical support; and Steve Deverel at Hydrofocus for site information.

PREFACE

The California Energy Commission Energy Research and Development Division supports public interest energy research and development that will help improve the quality of life in California by bringing environmentally safe, affordable, and reliable energy services and products to the marketplace.

The Energy Research and Development Division conducts public interest research, development, and demonstration (RD&D) projects to benefit California.

The Energy Research and Development Division strives to conduct the most promising public interest energy research by partnering with RD&D entities, including individuals, businesses, utilities, and public or private research institutions.

Energy Research and Development Division funding efforts are focused on the following RD&D program areas:

- Buildings End-Use Energy Efficiency
- Energy Innovations Small Grants
- Energy-Related Environmental Research
- Energy Systems Integration
- Environmentally Preferred Advanced Generation
- Industrial/Agricultural/Water End-Use Energy Efficiency
- Renewable Energy Technologies
- Transportation

Assessing the role of winter flooding on baseline greenhouse gas fluxes from corn fields in the Sacramento – San Joaquin Bay Delta is the final report for the study of greenhouse gas emissions on Staten Island project (contract number 500-09-012) conducted by U.S. Geological Survey. The information from this project contributes to Energy Research and Development Division's Energy Related Environmental Research Program.

For more information about the Energy Research and Development Division, please visit the Energy Commission's website at www.energy.ca.gov/research/ or contact the Energy Commission at 916-327-1551.

ABSTRACT

This study investigated the carbon dioxide (CO_2) and methane (CH_4) emission rates from agricultural operations (corn production) on peat soils in the Sacramento-San Joaquin Delta. Baseline data were obtained at, and comparisons made between, two representative corn fields on Staten Island in San Joaquin County, California with different winter management techniques: leaving the field fallow, or dormant, and intentional winter flooding. The baseline data will inform future projects designed to reduce net greenhouse gas (GHG) emissions in the Delta, which may result in low cost offsets for energy utilities that are part of the Cap-and-Trade program. Winter flooding is used by land managers to reduce erosion, improve soil texture, and provide habitat for water fowl, but may also lead to higher production rates of CH_4, with an accompanying increase in the global warming potential of the total emissions.

High winter GHG fluxes were measured at the flooded and non-flooded-treatment sites, with the measured CH_4 flux at the flooded site an order of magnitude greater than the non-flooded site and high in comparison to other published studies from similar environments. During the flooding period, the peat soils CO_2 fluxes were reduced, consistent with the management goal of reducing oxidative loss of soil organic material. On an annual basis, the CO_2 emitted from the two treatments was similar; however, the relative timing of CO_2 fluxes differed, with the flooded-treatment site having lower fluxes during the flooded period and higher fluxes during the non-flooded period (particularly during the transitional period following flooding). Soil temperature was the most significant driver for both CH_4 and CO_2 fluxes, and the data suggests that CH_4 emission levels of the flooded treatment might be lowered by altering the timing of flooding. This study highlights the importance of understanding how Delta agricultural land and water management can affect GHG emissions.

Keywords: carbon dioxide, methane, greenhouse gas emissions soil organic material, Sacramento-San Joaquin Delta

Please use the following citation for this report:

Pellerin, Brian; Frank Anderson; Brian Bergamaschi. (U.S. Geological Survey). 2014. ***Assessing the Role of Winter Flooding on Baseline Greenhouse Gas Fluxes from Corn Fields in the Sacramento – San Joaquin Bay Delta.*** California Energy Commission. Publication number: CEC-500-2014-077.

TABLE OF CONTENTS

Acknowledgements i

PREFACE ii

ABSTRACT iii

TABLE OF CONTENTS iv

LIST OF FIGURES v

LIST OF TABLES vi

EXECUTIVE SUMMARY 1

Introduction 1

Background and Overview 1

Project Objectives 2

Project Methods 2

Project Results 3

Benefits for California 3

CHAPTER 1: Introduction 6

CHAPTER 2: Study Site and Methods 8

2.1 Regional Characteristics 8

2.2 Site Description 9

2.3 Instrumentation 13

2.4 Flux Measurements 16

2.5 Energy Balance 16

2.6 Gas Sampling and Isotope Analysis 17

2.7 Soil Sampling Procedures 17

2.8 Data Analysis and Statistical Treatments 18

CHAPTER 3: Results 19

3.1 Site Conditions 19

3.2 CO2 Fluxes 23

3.2.1 Temporal Variability 23

3.2.2 Drivers 27

3.3 CH4 Fluxes 29

3.3.1 Temporal Variability 31

3.3.2 Drivers 32

CHAPTER 4: Discussion 34

CHAPTER 5: Conclusions 37

REFERENCES 39

APPENDIX A: A-1

Soil Chemical Properties A-1

Soil Isotopic Data A-2

Daily Eddy Flux and Meteorological Data A-2

LIST OF FIGURES

Figure 1: Delta map corn area, soil organic matter (percent) and study site (Staten Island). 11

Figure 2: Staten Island map with study sites. 12

Figure 3: Eddy covariance towers at the flooded treatment sites 13

Figure 4: Daily mean water table depths (meters) at both the flooded and non-flooded site compared with the total daily precipitation (millimeters) collected at the Twitchell Island CIMIS station. 20

Figure 5: Mean monthly precipitation and air temperatures from July 2011 through June 2013 compared to the mean climatic precipitation and air temperatures from 1997 to 2013. 21

Figure 6: Net ecosystem exchange from both the flooded and non-flooded site. 26

Figure 7: Soil isotopic values ($\delta^{13}C$ and $\delta^{15}N$, ‰) by site and depth, as well as isotopic values from corn biomass collected prior to harvest. 28

Figure 8: Regression analysis to determine the relationship between NEE and soil temperature under varying hydrological and field conditions. 28

Figure 9: Daily mean CH_4 flux from both the flooded and non-flooded site. 30

Figure 10: Mean daily CH_4 fluxes plotted together with mean daily soil temperatures 33

Figure 11: Mean daily CO_2 and CO_2-equivalent CH_4 fluxes compared against the mean daily soil temperature at the flooded site. 36

LIST OF TABLES

Table 1: Instrument and field operation timeline 15

Table 2: Mean daily solar radiation, air temperature, and wind speeds measured at the non-flooded site 22

Table 3: Mean soil conditions for both the flooded and non-flooded sites 22

Table 4: Summary of published winter carbon fluxes. Highest rates of CO_2 fluxes listed first, followed by CH_4 fluxes. 25

Table 5: Regressions comparing CO_2 (g-C m^{-2} d^{-1}) fluxes measured at the flooded and non-flooded site with environmental variables, energy fluxes, and carbon fluxes. 29

Table 6: Regressions comparing CH_4 (g-C m^{-2} d^{-1}) fluxes measured at the flooded and non-flooded site with environmental variables, energy fluxes, and carbon fluxes. 31

Table 7: CH_4 versus mean daily soil temperatures for varying hydrological and field conditions. 33

EXECUTIVE SUMMARY

Introduction

For this study, the research team assessed the baseline greenhouse gas (GHG) emissions from corn fields located on peatlands in the Sacramento – San Joaquin Bay Delta (Delta) under two winter field management techniques– conventional fallowing (the land is tilled and left unseeded or dormant for a season) and winter flooding. This project investigated whether winter flooding stimulates the production of methane (CH_4) gas, which has 25 times the global warming potential of carbon dioxide (CO_2). In addition, the study provides critical baseline GHG fluxes that could be used to inform policy actions related to land use and restoration in the Delta.

The release of GHG from peat soils in the Delta is currently thought to be a significant source of global warming potential (GWP) to the atmosphere, representing about three percent of California's total GHG emissions (including energy and transportation sector emissions). Accurate assessment of current emission rates are needed to further evaluate management practices that reduce GHG emissions, as well as the implications of converting agricultural lands to wetlands at a large scale. Although previous work has shown that that agricultural operations on peat soils lead to elevated release of CO_2, the extent to which intentional winter flooding affects soil oxidation and CH_4 productions has been previously uncharacterized. The central hypothesis guiding the study was that winter flooding would result in diminished oxidative loss of soil. This diminished oxidative loss would decrease the net annual CO_2 flux, but lead to production of CH_4 under the consequent anaerobic conditions in comparison to simply fallowing the land over winter.

The baseline data will inform potential future projects designed to reduce net greenhouse gas (GHG) emissions in the Delta, which may result in low cost offsets for energy utilities that are part of the cap-and-trade program.

Background and Overview

Peat soils have been widely drained and put into agricultural production due to their high fertility, which has altered their carbon budgets and GHG emissions. Establishing baseline emissions requires a clearer understanding of the driving factors – natural and anthropogenic – that affect both the timing and magnitude of CO_2 and CH_4 emissions to the atmosphere over seasonal to annual time scales. Although previous studies have focused principally on processes during the growing season, it is important to also understand fluxes during the uncultivated period. This is particularly true in temperate and tropical regions where soil microbial activity may remain high because winter temperatures are well above freezing.

Wintertime flooding of agricultural peatlands is an increasingly common practice in the Delta. Winter flooding is practiced on nearly 10 percent of Delta agricultural lands, with corn fields accounting for almost 80 percent of that winter flooded landscape. Flooding is thought to have many benefits, including mitigation of oxidative loss of peat soils, reduced erosion, improved soil texture, weed control, increased remineralization of crop residue, reduced pumping costs, and it permits the fields to serve as habitat for migratory waterfowl such as sand hill cranes.

Previous studies in agricultural fields and wetlands have shown that soil moisture and temperature are key determinants of GHG emission rates and fluxes from soils. For example, rice field and wetland studies have reported high fluxes of CH_4 due to changes in soil oxygen concentrations and redox conditions during long-term inundation (water coverage). Therefore, a critical first step in quantifying the baseline GHG emissions from peat soils in agricultural production is to develop a clearer understanding of the relationships between GHG emissions and the timing, duration and seasonality of soil saturation and flooding.

Project Objectives

This study (1) evaluated changes in the timing and magnitude of CO_2 and CH_4 fluxes from Delta corn fields under intentional winter flooding; (2) compared GHG fluxes from winter flooded fields to those using conventional fallowing, (3) assessed the drivers and management actions that may reduce GHG fluxes from these systems; and (4) provided a dataset of input and calibration/validation parameters for modeling the role of winter flooding and other hydrologic alterations on GHG fluxes from Delta agricultural fields. This represents a step towards developing a broader understanding of the timing, magnitude and variability of GHG release from Delta ecosystems, and fills a critical gap inthe baseline understanding of the Delta ecosystem.

Project Methods

We measured CO_2 and CH_4 flux continuously at the ecosystem-scale based on atmospheric measurements using the eddy covariance technique (EC). The EC technique is a statistical approach to measure the turbulent exchange of mass and energy between the atmosphere and vegetative surfaces. EC uses high frequency measurements (10 Hz) of scalars, such as temperature or CO_2, and vertical wind speeds within atmospheric boundary layer turbulent eddies to estimate energy and gas fluxes. EC is commonly used to estimate such parameters as heat, water, CO_2 and CH_4 such that daily, seasonal, and event-driven variability can be assessed.

CO_2 and water vapor (latent heat flux density) fluxes were measured using an open-path, infrared spectrometer in conjunction with vertical wind perturbation measurements from a sonic anemometer. An open path methane analyzer was used to measure CH_4 gas with the same vertical wind perturbation from the sonic anemometer to calculate the flux. The sensible

heat flux density was calculated from the covariance between perturbations in the sonic temperature and vertical velocity (both a product of the sonic anemometer). Mean daily fluxes of CO_2 and CH_4 were calculated for the entire measurement period by averaging the half-hour flux values.

Net radiation was measured using a four channel Kipp and Zonen net radiometer equipped with pyranometers for measuring solar radiation and pyrgeometers for measuring terrestrial radiation. Ground heat flux was calculated from the soil temperature profile. Water levels were monitored with Solinst Leveloggers (Model 3001) located in hand augered wells approximately 3.5 m deep. Many additional ancillary soil and gas samples were collected and analyzed.

Project Results

High winter GHG fluxes were measured at both the flooded and non-flooded-treatment sites. The measured CH_4 flux at the flooded site was an order of magnitude greater than the non-flooded site and high in comparison to other published studies from similar environments. The flooding of peat soils was found to reduce CO_2 fluxes during the flooded period, consistent with the management goal of reducing oxidative loss of soil organic material. However, this effect was largely confined to the periods of flooding. On an annual basis, the CO_2 emitted from the two treatments was similar; however, the relative timing of CO_2 fluxes differed, with the flooded-treatment site having lower fluxes during the flooded period and higher fluxes during the non-flooded period (particularly during the transitional period following flooding).

Soil temperature was found to be the most significant driver for both CH_4 and CO_2 fluxes in both fields and for both periods during which anaerobic and aerobic soil respiration were occurring. Expressed in CO_2-equivalent mass units, the fallow-treatment site total GHG release was 21.2 MT CO_{2e} $ha^{-1}yr^{-1}$ while the flooded-treatment site total GHG release was estimated to be 25 MT CO_{2e} $ha^{-1}yr^{-1}$ when both the grain production and loss through the hydrologic system are included.The data suggests that CH_4 emission levels of the flooded treatment might be lowered by altering the timing of flooding. For example, a delay in flooding until soil temperatures decrease could potentially reduce the amount of CH_4 emitted by nearly half, providing a relatively simple management practice to mitigate the effects of GHG release from intentionally flooded landscapes sites. However, the potential for increased GHG emissions from Delta peatland agricultural landscapes due to projected increases in night-time temperatures and elevated CH_4 fluxes from winter-flooded fields may affect the magnitude of the flux.

Benefits for California

This work has the potential to benefit the state of California by (1) identifying opportunities for reduction of GHG emissions from Delta peatland agricultural landscapes. Furthermore, this

project will serve by (2) informing policymakers about the potential value and tradeoffs of changing land use and management practices on Delta agricultural peatlands, including the tradeoffs in GHG benefits that may occur with large scale restoration of wetlands in the Delta as mandated by the current Bay Delta Conservation Plan draft. Moreover, this work has the potential to (3) provide baseline GHG flux data to evaluate land management practices aimed at biomitigation of atmospheric levels of CO_2 and low cost offsets for energy utilities in programs such as California's Carbon Cap and Trade program, benefiting California ratepayers.

CHAPTER 1: Introduction

Restoration of sites historically characterized by the formation of peat and carbon-rich soils represents a significant global opportunity for the biological mitigation of rising greenhouse gas (GHG) concentrations in the atmosphere. This effort has largely focused on tropical and temperate settings where the longer growing season results in more rapid accumulation of organic material and where warmer winter temperatures extend the period of high soil microbial activity (Miller, 2008). However, a clear understanding of emissions under current management is crucial to evaluating the effects of restoration or management on GHG emissions. For example, evaluations of the benefits in carbon offset programs such as the State of California's Cap-and-Trade market are based on the verifiable difference between current (or baseline) emissions and emissions following management conversion.

Carbon-rich peat represents an interesting and important hydrogeomorphic class of soils that have been significantly impacted by agricultural management activities in California and elsewhere (Drexler et al., 2009a, b; Deverel and Rojstaczer, 1996; Kasimir-Klemedtsson et al., 1997). In particular, peat soils in the Sacramento – San Joaquin Delta have been widely drained and put into agricultural production since the mid-1800s due to high soil fertility, resulting in subsidence of up to 8 meters due to the oxidation of peat (Deverel and Leighton, 2010). Studies of GHG emissions in the Delta typically focus on either differences between crop types and cropping systems (De Gryze et al., 2010), or the impact of flooding for rice or wetlands (Miller, 2008; Hatala et al., 2012).

Seasonal flooding of fallow agricultural fields is a relatively common practice in the California Central Valley and Delta that may significantly alter GHG emissions. Flooding is intended to mitigate oxidative loss of peat soils, reduce erosion, improve soil texture, suppress weed growth, promote remineralization of crop residue, reduce pumping costs, and, in many cases, permit the fields to serve as habitat for migratory waterfowl (Ivey et al., 2003). Previous studies in agricultural fields and wetlands have shown that soil moisture is a key determinant of GHG emission rates and fluxes from soils. For example, rice and wetland studies have reported high fluxes of methane (CH_4) due to changes in soil oxygen concentrations and redox conditions during long-term inundation (Li et al., 2005). Similarly, anaerobic conditions brought about by soil saturation resulted in a significant flux of nitrous oxide (N_2O), particularly during transition periods such as flood up and drawdown (Li et al., 2005). Therefore, a critical first step in quantifying the baseline GHG emissions from peat soils in agricultural production is to develop a clearer understanding of the relationships between GHG emissions and the timing, duration and seasonality of soil saturation and winter flooding. This is particularly important in

Mediterranean climates such as California where soil microbial activity may remain high because winter temperatures are well above freezing.

In addition to soil moisture, the magnitude and timing of GHG fluxes from agricultural landscapes is influenced by soil tillage practices, cover cropping, crop residue management and fertilizer applications (De Gryze et al., 2010; Li et al., 2005). For example, studies have reported that changes in soil organic carbon content and the addition of nitrogen fertilizer strongly influence GHG fluxes from agricultural soils (Lee et al., 2006; Bouwman et al., 2002). Several biogeochemical parameters related to land use – along with the timing, frequency and duration of soil saturation – likely influence the GHG fluxes from peat agricultural soils. Additional data are needed for field and modeling studies to assess if management approaches meet multiple objectives including carbon storage, agricultural productivity, and broader ecosystem services such as waterfowl habitat.

The U.S. Geological Survey assessed the baseline GHG emissions from harvested corn fields on peat soils in the Sacramento – San Joaquin Bay Delta, a region of highly subsided peat-rich islands. Policy makers are actively considering incentives for improving management practices to limit GHG emissions as well as conversion of agricultural lands to wetlands at a large scale. To evaluate the impact of policy choices on GHG emissions, an accurate assessment of current emission rates is needed. Although it is relatively widely accepted that agricultural operations on peat soils leads to elevated release of carbon dioxide (CO_2), the extent to which flooding management affects soil oxidation and CH_4 productions has been previously uncharacterized. The team hypothesized that the flooding treatment would result in diminished oxidative loss of soil. This in turn would decrease the net annual CO_2 flux, but production of CH_4 under the consequent anaerobic conditions would result in a greater global warming potential in comparison to simply fallowing the land over winter.

CHAPTER 2:
Study Site and Methods

2.1 Regional Characteristics

The Delta comprises approximately 750,000 acres of peat-rich islands, with approximately 500,000 acres under agricultural production (http://ucanr.edu/sites/deltacrops/; last accessed on Sept. 28, 2013). Approximately two thirds of the peat soils once extant on farmed areas of the Delta have been lost due to drainage, mechanical disturbance, and subsequent microbial oxidation (Drexler et al. 2009b; Deverel and Leighton, 2010). Consequently, over 70 percent of the Delta is below sea level.

Staten Island (38°10'29"N, 121°30'17"W) was chosen for the study due to its proximity within a large corn growing region in the Delta (**Figure 1**). Corn production is a common and increasing agricultural land use in the Delta, accounting for nearly 20 percent of the agricultural land use today (http://ucanr.edu/sites/deltacrops/; last accessed on Sept. 28, 2013). Corn in this region of the Delta is typically planted in April or May, depending on patterns of precipitation and temperature for the specific year and a small fertilizer application is typically applied during planting. Fields were irrigated during the growing season two times using spud ditches, depending on local temperatures and precipitation. Harvest generally occurs in October.

Winter flooding of agricultural fields has occurred for more than 60 years in the Delta in part to provide wintering areas for migratory birds on the Pacific Flyway (Delta Protection Commission, 1994). In the Delta, harvested corn fields make up nearly 80 percent of the total winter flooded area (37,236 acres), an area equivalent to approximately 25 percent of the total area planted in corn in the basin (Central Valley Joint Venture, 2006). Fields designated for flooding are typically inundated from October to February and serve as a particularly important habitat for sand hill cranes (Pogson and Lindstedt, 1991).

The climate in the Delta is classified as Mediterranean, with warm, dry summers and cool, moist winters, providing a long growing season for both agricultural and natural systems. However, relatively little precipitation falls during the peak growing season; irrigation from surrounding rivers and sloughs is needed to maintain positive water budgets for agricultural production. Air temperature and precipitation data used for this study was recorded at a local climate station on Twitchell Island (approximately 10 km to the southwest of Staten Island; California Irrigation Management Information System (CIMIS): http://wwwcimis.water.ca.gov/cimis/). The mean air temperature and annual precipitation at the Twitchell Island CIMIS station from October 1997 to June 2013, was 15.0 °C and 328.1 mm, respectively. Longer climate records collected at the Antioch climate station (1949 -1999) show little difference from the Twitchell Island data, where the annual mean temperature and

precipitation was 15.1 °C and 335 mm, respectively (Hatala et al., 2012). The mean minimum monthly temperature (4.6°C) occurs in January and the mean maximum monthly temperature (24.1°C) occurs in July. December, January, and February have the highest monthly precipitation averages with a combined total of ~180 mm or over half of the mean annual precipitation.

Weather in the Delta is greatly influenced by the surrounding topography and the influence of the semi-permanent Pacific High pressure system. A break in the Coastal mountain range to the west, not only allows the waterways of the Delta to drain into San Francisco Estuary, but also allows the mixing of air masses between the Pacific Ocean and the Sacramento and San Joaquin valleys (Figure 1). The Pacific High often dominates the summer weather pattern in the region, causing daytime high temperatures to often exceed 38°C in the Sacramento and San Joaquin Valleys. However, the Delta is often cooled by moist afternoon breezes that filter into the region from the Pacific Ocean, known locally as the "Delta Breeze". This localized weather pattern is not considered a true land-sea breeze interaction but is the result of the changing position of the Pacific High pressure system in the Eastern Pacific Ocean and the formation of fog near the California coast. The Mediterranean climate of the Delta, together with the "Delta Breeze", creates conditions for high plant productivity during daylight hours and limits respiration during the cool nighttime hours. The "Delta Breeze" facilitates flux measurements because they increase turbulence, resulting in fewer periods of unresolvable gas fluxes.

In the winter, the Delta region is impacted by the interaction between the Aleutian low and the semi-permanent Pacific high-pressure systems. Southeasterly airflow that precedes low-pressure systems funnels through the break in the Coastal range, similar to the summer "Delta Breeze" conditions, and cool, moist air influences the Delta region. Wind flow behind the passage of low-pressure system comes from the North and the wind direction as well as magnitudes is enhanced as the air travels along the eastern edge of the Coastal range. Under these conditions, vapor pressure drops and in the winter the air temperatures are usually cool. If these conditions occur in the fall and spring, the air mass will be dry but sometimes heated by adiabatic (downsloping winds) and diabatic (insolation) conditions. When the Pacific high dominates the air mass in the winter, atmospheric conditions are normally calm and fog forms in the valleys and Delta. Under these conditions, winds in the Delta flow to the west out to the San Francisco Bay. Fog in the Delta can persist for days and even weeks, but occurrence in recent years have declined (Baldocchi and Waller, 2012). During the study, all of the aforementioned weather scenarios occurred and influenced energy and carbon fluxes.

2.2 Site Description

Two field study sites were selected on Staten Island (38°10′29″N, 121°30′17″W) in the Sacramento-San Joaquin Delta (hereafter, the Delta) (**Figure 2**) to compare the GHG emissions

from winter flooding and **conventional r fallow treatments**. Staten Island is owned and managed by The Nature Conservancy. It is approximately 9,200 acres in size and roughly 8,400 of which for the last 25 years have been dedicated to growing corn and winter wheat (Ivey et al., 2003). The subsidence of peat soils on Staten Island has reduced mean land elevations to 8 meters below sea level (Deverel and Leighton, 2010). About one-third of the island is flooded in the winter to reduce erosion, control weeds, improve soil texture, and provide an important habitat for overwintering sand hill cranes and other waterfowl.

The sites were located in the center of Staten Island, where peat is approximately 2 meters thick, percent organic matter of the soil typically ranges from 20 to 30percent and land elevation is about 3.8 meters below sea level (Deverel and Leighton, 2010). Eddy covariance (EC) towers were established at the two study sites approximately one kilometer apart (**Figs. 2, 3**). Selection of these sites was intended to permit comparison of GHG fluxes from the flooded and non-flooded treatments and to reduce the influence of other potential confounding influences.

The flooded-treatment site is on the western side of the island and is classified by three soil types: Ryde Clay Loam, Peltier Mucky Clay Loam, and Rindge Muck; where the reference site is on the eastern side of the island is classified by three soil types: Peltier Mucky Clay Loam, Rindge Muck, and Rindge Mucky Silt Loam (USDA SCS, 2003). The site locations were chosen for similarity in original soil type, climate, and historical consistency of crop management. Crop management has been consistent at both sites for the past 25 years (personnel communication, Brent Tadman, Land Manager, The Nature Conservancy). During the summer, both sites were farmed for corn under the same management regime (i.e., same field operations, irrigation events, seed stock, etc.), while in the winter, one site was flooded (flooded-treatment site) and the other site was left fallow (non-flooded-treatment site).

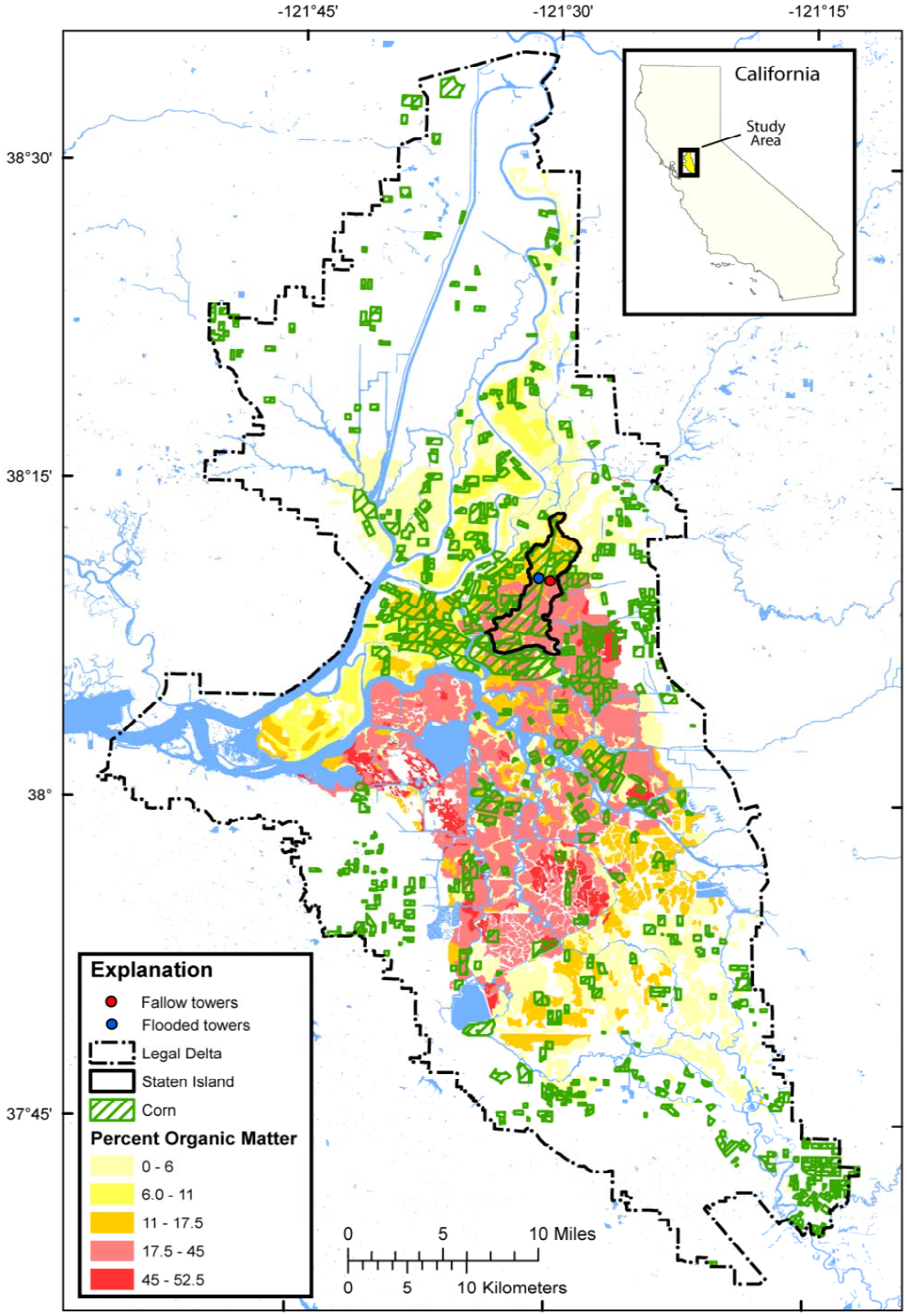

Figure 1: Delta map corn area, soil organic matter (percent) and study site (Staten Island).

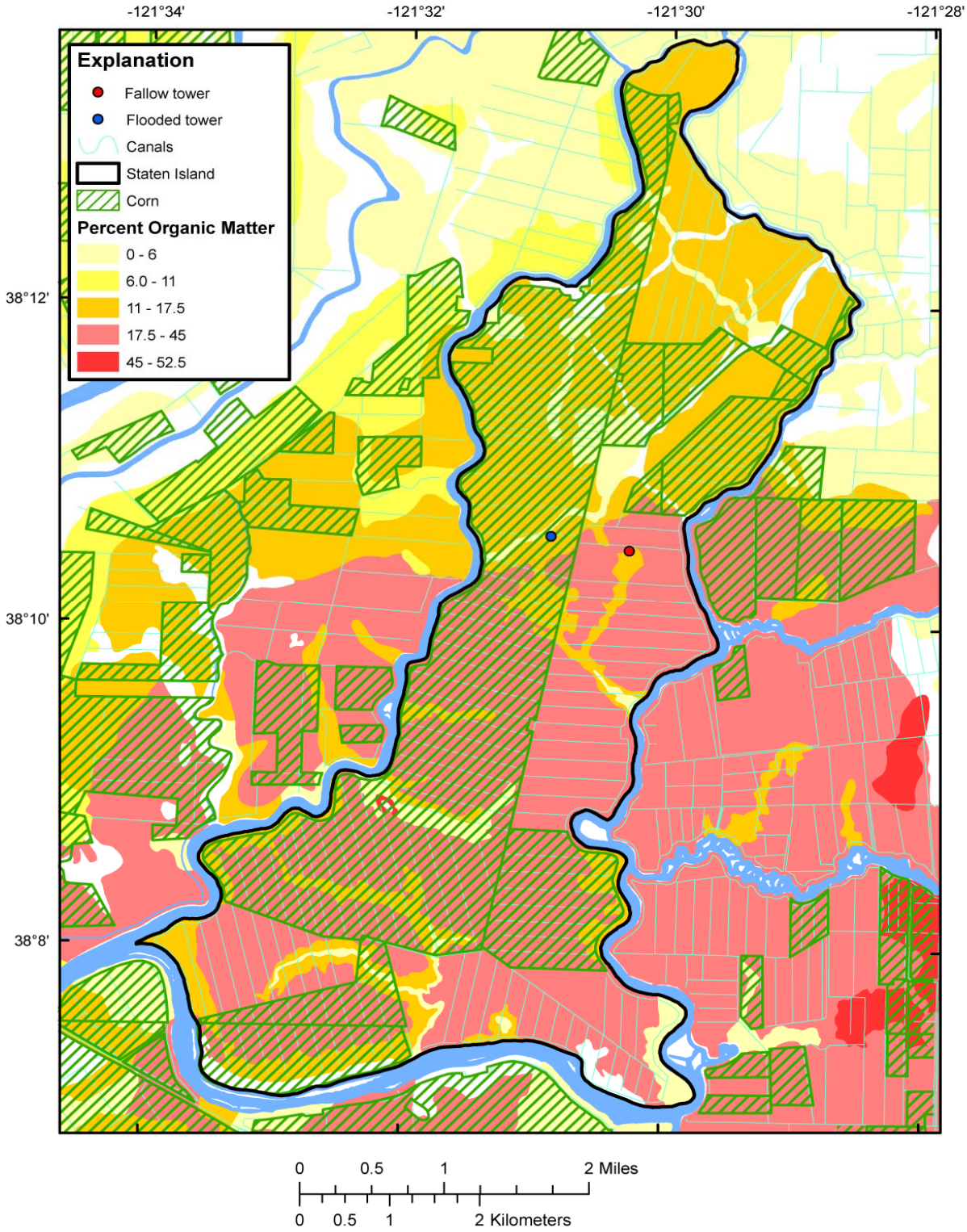

Figure 2: Staten Island map with study sites.

Figure 3: Eddy covariance towers at the flooded treatment sites

(left) and non-flooded treatment site (right). Water Table Depth

Shallow wells were installed at both the flooded- and fallow-treatment flux tower locations on 7/19/2012 to provide data on fluctuations in water table depth. The wells were hand-augered using a 22 cm bucket auger and constructed using 5.1 cm diameter PVC pipe. A 10.2 cm pointed cap was attached to the bottom of a 3.0 meter length of 0.5 mm screened pvc pipe, followed by a 1.5 meter section of non-screened pvc pipe. Wells were approximately 3.5 meters deep. Well casings were packed with #3 size silica sand to approximately 15 cm from the soil surface and sealed using medium chip Bentonite.

Both wells were instrumented with Solinst Leveloggers Model 3001 approximately 0.7 meters from the bottom. The Levelogger readings have a water level accuracy of ± 0.05percent FS and were corrected for pressure using a Solinst Barologger model 3001 (pressure accuracy of ± 0.05 kPa). The Leveloggers were cleaned and data was downloaded approximately every two weeks. Ground water levels were never lower than two meters below the surface at either site and at the flooded-treatment site, the water level reached approximately 0.6 meters above the surface during the 2012/2013 winter. Water levels were always within or above the screened portion of the well.

2.3 Instrumentation

The following meteorological instrumentation was installed at each site on a 4.3 meter tower from Scaffoldmart (Greenville, NC, USA): a four component net radiometer, installed at 4.3 meters (CNR1; Kipp and Zonen, Delft, Netherlands); up- and downward facing quantum sensors, installed at 4.3 meters (LI190; LI-COR Biogeosciences, Lincoln NE, USA); water content reflectometer, installed at a depth of 0 – 30 cm (CS616; Campbell Scientific, Logan, UT, USA), 2-

ground heat flux plates, installed at depth of 5 cm (REBS Heat Flux Plates; Campbell Scientific, Logan, UT, USA); 4-soil thermocouples, installed at a depth of 5 cm (TCAV Averaging Thermocouple; Campbell Scientific, Logan, UT, USA); and camera set to take pictures every day at noon (Plantcam; Wingscapes, Alabaster, AL, USA). At the fallow treatment site, the team installed a direct and diffuse radiometer (SPN1 Sunshine Pyranometer; Delta-T Devices Ltd., Burwell, Cambridge, UK) and during the first winter at the flooded site, the team installed a pressure transducer to measure water levels (WL400 Water Level Sensor; Global Water Instrumentation, Inc., Gold River, CA, USA). All meteorological data was sampled every minute and half-hour means were stored on Campbell Scientific dataloggers (2-CR1000s at the flooded treatment site, and a CR23X with an AM16/32 Multiplexer at the fallow treatment site). On a daily basis, data was transmitted remotely from the towers to a central server housed at the USGS office (Placer Hall-CSUS, Sacramento, CA, USA), where daily reports were created and checked for instrument malfunction. Both sites were powered remotely using 3-125 watt solar panels (Kyocera, Scottsdale, AZ, USA), 8-225 Ah @ 20 hr rate, 6 volt Batteries (Crown Battery, Fremont, OH, USA) and regulated by a ProStar 30 amp 12/24 volt solar charge controller, with digital meter (Morningstar, Newtown, PA, USA).

At both sites, eddy covariance instrumentation was installed at approximately 4.1 meters, which included: athree-dimensional sonic anemometer (Gill Windmaster; Gill Instruments Ltd, Lymington, Hampshire, UK or RM Young 81000, Traverse City, MI, USA); an open-path, infrared spectrometer (LI-7500; LI-COR Biogeosciences, Lincoln, NE, USA); and open- path methane analyzer (LI-7700; LI-COR Biogeosciences, Lincoln, NE, USA); and aspirated air temperature and relative humidity (HMP45C ; Vaisala, Vantaa, Finland). The raw 10 Hz data were collected and stored using Campbell Scientific's CR1000 datalogger with a card reader (CFM; Campbell Scientific, Logan, UT, USA). The LI-7500 and LI-7700 were calibrated approximately every three months using NIST traceable CO_2 and CH_4 gases. The team used N_2 (5.0 purity; Praxair, Sacramento, CA, USA) for the zero calibration gas and dew point temperatures were generated from a portable dew point generator (LI-610; LI-COR Biogeosciences, Lincoln) to calibrate the water vapor component of the LI-7500. To be consistent between the two study sites, th team removed the RM Young three-dimensional sonic anemometer that was originally installed at the flooded treatment site in mid-April and replaced it with a Gill Windmaster three-dimensional sonic anemometer (**Table 1**). Unfortunately, the Gill Windmaster had an instrument malfunction and reported dampened vertical wind speed data from installation in mid-April to October. In October, the original RM Young three-dimensional sonic was installed next to the Gill and data was collected from both sonic anemometers for the duration of the study (i.e. October 2012-May 2013). The team corrected the erroneous Gill data (mid-

April through October), using a simple linear regression from the side by side comparison for all the fluxes: CO_2, CH_4, latent energy flux and sensible heat flux.

Table 1: Instrument and field operation timeline

Where "X" indicates a full month of operation, ">" indicates the first half of the month is in operation and "<" indicates the last half of the month is in operation. "H" represents the month in which corn harvest took place and "P/F" is the month when the field was planted and fertilizer was applied. The numbers in the irrigation/flooded row indicate the number of irrigation events, while "X" or ">/<"is when the flooded treatment was flooded.

Site	Instruments	O, 11	N, 11	D, 11	J, 12	F, 12	M, 12	A, 12	M, 12	J, 12	J, 12	A, 12	S, 12	O, 12	N, 12	D , 12	J, 13	F, 13	M, 13	A, 13	M, 13
Flooded	RMY Sonic	<	X	X	X	X	X	>						X	X	X	X	X	X	X	>
	Gill Sonic							<	X	X	X	X	X	X	X	X	X	X	X	X	>
	Energy/Meteorology	<	X	X	X	X	X	X	X	X	X	X	X	X	X	X	X	X	X	X	>
	CO_2/H_2O	<	X	X	X	X	X	X	X	X	X	X	X	X	X	X	X	X	X	X	>
	CH_4		X	X	X	X	X	X	X	X		>	<	<	X	X	X	X	X		>
	Water Table Depth				<	X	X				<	X	X	X	X	X	X	X	X	X	>
Fallow	Gill Sonic							<	X	X	X	X	X	X	X	X	X	X	X	X	>
	Energy/Meteorology							<	X	X	X	X	X	X	X	X	X	X	X	X	>
	CO_2/H_2O							<	X	X	X	X	X	X	X	X	X	X	X	X	>
	CH_4										X	<	>	>	X	X	X	X		X	
	Water Table Depth										<	X	X	X	X	X	X	X	X	X	>
Corn	Plant	H						P/F	X	X	X	X	H							P/F	X
	Irrigation/Flood		X	X	X	>				1<	2	2		<	X	X	X				

2.4 Flux Measurements

Fluxes of CO_2, CH_4 and energy were measured at the flooded treatment site from late-October 2011 to mid-May 2013, while at the fallow treatment site; from late-April 2012 through mid-May 2013 (**Table 1**). Fluxes were calculated based on the eddy covariance technique (EC), which uses a statistical approach to measure the turbulent exchange of mass and energy between the atmosphere and vegetative surfaces (Aubinet et al., 2012). Half-hour fluxes are computed from the perturbation of high frequency (10 Hz) measurements of temperature or gas concentrations with the perturbations in vertical winds for each half-hour. As part of the post-processing calculation, the raw 10 Hz data goes through a series of corrections that include: (1) the despiking of the raw data (eliminating any data outside six standard deviations for a one-minute moving window); (2) the determination of the lag in time created by the separation of the eddy covariance instrumentation, changes in wind speed and direction, and signal processing; (3) coordinate rotation to align the local mean wind vector with the x direction in the Cartesian coordinate system, correct any misalignment of the vertical wind component, and correct for humidity effects upon the sonic anemometer (Schotanus et al. 1983), (4) correct for air density fluctuations or the Webb-Pearman-Leuning correction (WPL; [Webb et al., 1980]), and (5) stationarity.

After the calculation of the half-hour fluxes, the results are further filtered for: (1) turbulent conditions that are too low to accurately assess the turbulence ($u^*<0.05$) or unrealistically high turbulent conditions ($u^*>1.2$); (2) fluxes that are outside what is realistically expected; and (3) wind directions that come from the tower (azimuth wind directions: 15-90° for both sites). Fluxes were then gap-filled following Reichstein et al. (2005) methodology that uses time and fluxes under similar meteorological conditions (solar radiation, air temperature, and vapor pressure deficits) to replace the missing half-hour data. The gap-filling algorithm uses both changes in time (i.e. ± 7 days, ±14 days, and ±28 days) and available meteorological data to classify the quality of the flux used to gap fill. Less than 50percent of all the CO_2 and energy fluxes were gap-filled and fall within the acceptable percentage of missing data among other flux studies (Moffat et al., 2007). The gap-filled data for CH_4 fluxes were higher for both the flooded and fallow treatments, as one LI-7700 was swapped between the two sites every 3-4 weeks from mid-April through October 2012. From 10/31/2012 through 3/5/2013 (our focused study period), an additional LI-7700 was acquired and concurrent measurements were taken at both sites. After 3/5/2013, one LI-7700 was again swapped between the sites.

2.5 Energy Balance

The half-hourly energy balance closure was calculated using an equal weight energy balance ratio approach similar to equation 2, in Wilson et al. (2002). The difference is that the team sums the diurnal average (not including storage) instead of taking all available measurements. The

effect of this approach is that it applies an equal weight to the energy balance at all times of day, eliminating any bias in missing data (typically at night) and not accurately accounting for energy storage on a half-hour time scale. Final calculations were accomplished by first building a matrix of half-hour sums of latent heat (LE) and sensible heat (H) fluxes, when both values were not missing, for entire study period. Half-hour means were calculated from all non-missing values for each half-hour and then summed for a total mean daily value. The same equal weight approach was used for net radiation (R_n) minus ground heat flux (G), and the energy balance closure was calculated as:

$$EB\ Closure = \frac{\sum(LE+H)}{\sum(R_n-G)} \times 100\% \quad (1)$$

Using this approach, hourly energy balance closure at the flooded site was 89.3percent when the field was flooded and 86.1percent when the water was drained from the field. At the non-flooded site, the energy budget closure was 66.1percent for the entire study period. The percentages at both sites are within the acceptable range of other FLUXNET network sites, but lower energy budget closure suggests possible lower rates of CO_2 fluxes (Wilson et al., 2002). Therefore the carbon fluxes presented here are a conservative estimate.

2.6 Gas Sampling and Isotope Analysis

Static greenhouse gas sampling chambers were installed to assess both the eddy covariance measurements and the spatial variability within the field sampling footprint. Samples were collected using a static chamber technique with samples collected at six locations per field at equally spaced time intervals (e.g. 0, 30, 60 minutes) to calculate gas fluxes. Samples were collected for analysis of concentrations (CO_2, CH_4 and N_2O) on a Shimadzu gas chromatograph (Model GC-2014) at UC-Davis and isotopic values (^{13}C, ^{15}N) on a ThermoScientific Delta V Plus isotope ratio mass spectrometer at the UC-Davis stable isotope facility.

Challenges with GHG sample collection preclude the straightforward interpretation of the concentration data. In particular, fans used to circulate air within the chamber caused the base to vibrate in the soft sediment of the flooded treatment and resulted the ebullition of gas bubbles into the chamber. This was a particular problem in the flooded fields, and data are therefore not discussed in this report. This also unfortunately precludes us from discussing N_2O dynamics, which was not measured on the eddy flux towers due to cost of acquiring a continuous N_2O analyzer for the study (<$100K).

2.7 Soil Sampling Procedures

Soil samples were collected at both the flooded- and fallow treatment fields at six locations within the measurement footprint of the flux towers. For each of the six locations, three 60 cm^3 samples from depths 0 to 10 cm, 10 to 20 cm, and 20 to 30 cm, were collected using a Madera

bulk density soil sampler and homogenized. Soil bulk density was assessed by weighing the homogenized samples before and after drying. Each of the homogenized samples were subsampled and analyzed for percent OM by loss on ignition.

2.8 Data Analysis and Statistical Treatments

Mean daily fluxes of CO_2 and CH_4 were calculated for the entire measurement period by averaging the half-hour flux values. Comparison of fluxes to field conditions and meteorological variables were conducted using these mean daily flux values. Conversion of C mass fluxes of CH_4 to CO_2-equivalent mass units used a GWP multiplier of 25.

To investigate the relationship between CO_2 flux and environmental variables during the time after harvest and before planting, the time series of CO_2 flux for both treatments was divided into two periods, approximately corresponding to when the flooded treatment was inundated and when it was drained. For the flooded treatment, the first period was from 10/31/12 to 2/9/13, and the second, drained period was from 2/10/13 to 3/5/13. For the fallow treatment, the first period was from 10/31/12 to 2/14/13 and the second period was from 2/15/13 to 3/5/13, when weeds were observed to be growing in the fallow-treatment field.

To investigate the relationship between CH_4 flux and soil temperatures during the fallow period, the time series of CH_4 flux collected at the flooded-treatment site was divided into four periods. The periods corresponded to changes in methane emissions or water management. The first period is the first emission peak of methane flux (10/31/12 to 1/4/13). The second period is corresponds to the second peak in CH_4 flux (1/5/13 to 2/1/13). The third period corresponds to the initial draining of the field (2/2/13 to 2/9/13). The fourth period corresponds to when the field was fallow and slowly drying out (2/10/13 to 3/5/13).

The two tailed t-test was used to identify significant differences between mean daily flux values for the following comparisons: (a) the flooded and fallow treatments sites for the entire study period; (b) the flooded and fallow treatments during the periods describe above; (c) the individual periods for each treatment. To compare CH_4 fluxes with soil temperatures at the flooded-treatment site, a one-way analysis of variance (ANOVA) was carried out for individual time periods. Finally, linear regression was used to assess the correlation between soil temperature and flux for the individual time periods.

CHAPTER 3: Results

This study examined the GHG emissions from corn fields on Staten Island under different winter water management (intentional seasonal flooding and fallow from 10/31/12 to 3/5/13) to: 1) provide baseline emissions data against which to evaluate the relative merits of various land management techniques and 2) permit comparison of net fluxes to other land uses such as pasture, rice, and re-established wetland. Further, this study examined processes driving CO_2 and CH_4 fluxes to permit future evaluation of temporal trends, model extrapolation to other sites and treatments, and explore how GHG fluxes might change under different environmental conditions and under projected future climate scenarios.

3.1 Site Conditions

There have been many studies investigating the relationship between environmental site conditions and carbon fluxes in sites with high peat soil content. Soil temperature and water table depth are often cited as the two most important (Moore and Dalva, 1993; Bubier et al. 2003; Fang and Moncrieff, 2001; Juszczak et al. 2013; and many others). Other potentially important drivers of energy and carbon fluxes include meteorologic conditions (Baldocchi et al., 2012) , turbulence (Friborg et al. 1997; Lai et al. 2012), photosynthetically-active radiation flux density (A. Lindroth et al. 2007; Miyata et al. 2000; and many others), soil organic matter content (Paustian et al., 1998), and plant biomass (Chanton et al. 1993, Bellisario et al. 1999; and many others).

At the outset of the flux-measurement period (10/31/12), water table depth at the fallow-treatment site was approximately one meter below the surface (**Figure 4**) and remained well below the surface for the entire study period. In the flooded-treatment site, water level was 0.3 m above the surface at the start of the study and increased from ~0.3 to ~0.5 meters above the surface (11/13/12) after additional water was applied. After 1/24/13, the water level at the flooded-treatment site dropped rapidly, and by 2/1/13, the water table was below the surface.

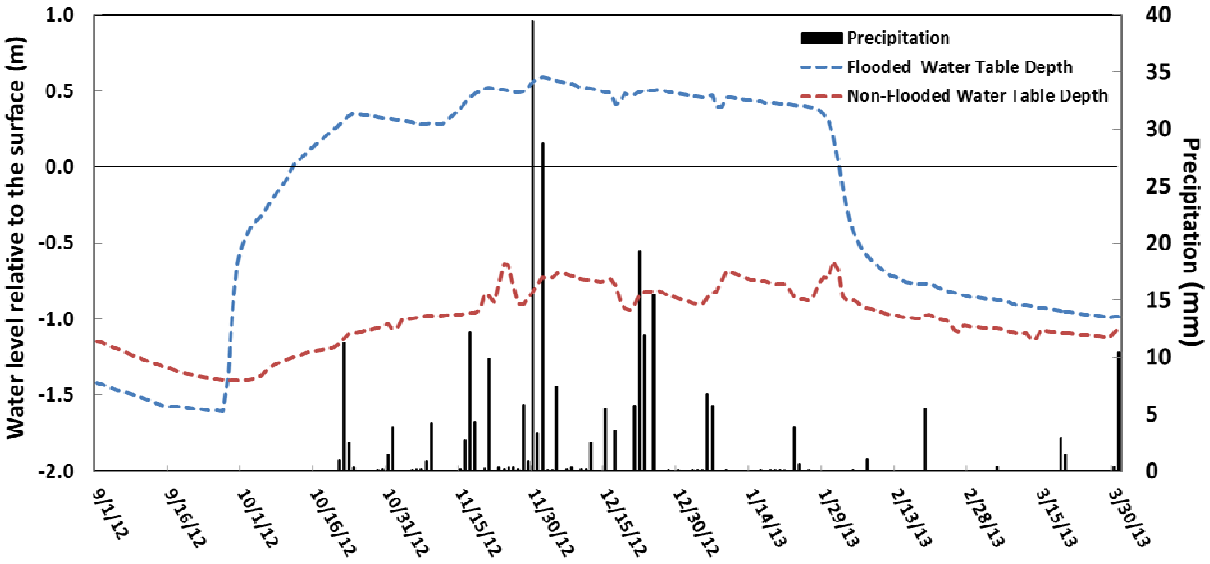

Figure 4: Daily mean water table depths (meters) at both the flooded and non-flooded site compared with the total daily precipitation (millimeters) collected at the Twitchell Island CIMIS station.

The winter carbon flux data presented in this study begins on 10/31/12 and goes through 3/5/13. The time series of water table depth and precipitation were extended to include the seasonal minimum at the both the flooded and non-flooded site.

Weather conditions at the treatment sites varied considerably over the study period. November and December were characterized by above average precipitation, air temperature, and wind speeds (**Figure 5, Table 2**). The cloudy conditions during this period kept mean daily air temperatures slightly above average (+14percent) and solar radiation near average. Dry, clear and cooler conditions prevailed in January and February, resulting in daily mean air temperatures slightly below average (-11percent) and above average (+43percent) daily mean solar radiation values.

Water table depth at both sites responded to precipitation events, which occurred mostly in the first half of the study period (**Figure 4**). In November and December of 2012, the Twitchell Island CIMIS station recorded 192.4 mm of rainfall, 59percent of the total amount of precipitation received for the 2012/2013 water year and 200percent of the climatic average (1997-2013). In contrast, the combined rainfall amount for January and February was 24.6 mm, just 21percent of the climatic average. At the flooded-treatment site, precipitation events generally induced immediate rises in water table depth. However, at the fallow-treatment site, not all precipitation events induced changes water table depth. Further, changes in water table depth were observed at the fallow-treatment site in the absence of rainfall, likely responding to water-management activity elsewhere on the island.

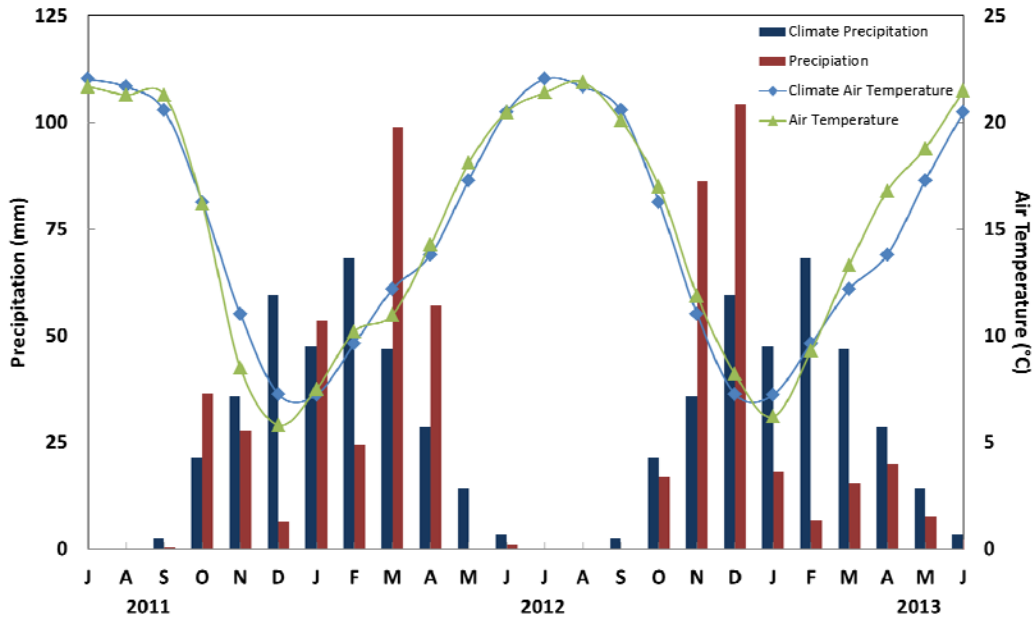

Figure 5: Mean monthly precipitation and air temperatures from July 2011 through June 2013 compared to the mean climatic precipitation and air temperatures from 1997 to 2013.

All values were measured by the Twitchell Island climate station as part of the California Department of Water Resources California Irrigation Management Information System (CIMIS). Air temperature and precipitation were below average in the fall of 2011, followed by above average precipitation in March of April of 2012. Precipitation was well above average in November and December of 2012, with slightly above average temperatures. Precipitation was below average for all months in 2013 and air temperatures were slightly below average in January and February, followed by average air temperatures March through June.

Mean soil temperatures were higher at the flooded-treatment site (10.7°C; **Table 3**) in comparison to the fallow-treatment site (8.8°C). There was a seasonal trend in soil temperatures at both sites, where magnitudes were higher in November and February and lowest in late December and early January (Figure 4). Soil temperatures in November-December were on average 2°C higher than January-February (Figure 4). Flooded conditions had a moderating effect on soil temperatures; the high heat capacity of the standing water kept mean daily minimum temperatures warmer than the soils at the fallow-treatment site. Once rainfall began in mid-November, soil temperatures at the fallow-treatment site increased for a few days following rainfall events. In these cases, the increase in surface soil moisture and cloud cover created conditions where soil temperatures became similar between the two sites.

Contrary to expectation and despite the careful site selection process, there were substantial differences in average bulk soil properties between sites. The mean OM content at the flooded-treatment site (9.8percent) was lower than the fallow-treatment site (25percent). The mean soil

bulk density at the flooded-treatment site was 0.93 g cm^{-3}, higher than that of the flooded-treatment site (0.57 g cm^{-3}; **Table 3**). The authors believe the average values from the flood-treatment site are somewhat skewed by the presence of sediments from a historic river channel in the composited material (S. Deverel, personal communication). Additional discrete sampling of soils (depth: 0-10cm) within the flux footprint yielded OM values ranging of 7.1 to 15.6percent and the bulk densities from 0.95 to 0.65.

No measurable change in these soil properties was observed for the study period (**Table 3**). It is not clear if the measured differences in these properties were related to intrinsic soil properties or historic differences in management practices of the two sites.

Table 2: Mean daily solar radiation, air temperature, and wind speeds measured at the non-flooded site

Presented as a study period mean value, a November-December mean value, and a January-February mean value. For the study period, the range between daily mean minimum and maximum are reported in the parentheses and for November-December and January-February, a comparison to the climatic mean is given in the parentheses.

	Solar Radiation (MJ/m2/d)	Air Temperature (°C)	Wind Speed (m s^{-1})
Study Period (10/31/12-3/5/13)	10.7 (range: 1.3-19.3)	9.0 (range: 2.1-16.4)	2.2 (range: 0.7-6.6)
November-December	8.4 (climate mean: 7.9)	10.0 (climate mean: 9.2)	2.4 (climate mean: 2.34)
January-February	12.7 (climate mean: 8.9)	7.5 (climate mean: 8.4)	2.0 (climate mean: 2.55)

Table 3: Mean soil conditions for both the flooded and non-flooded sites.

Both summer and winter organic matter (percent loss on ignition) show very little change from the winter treatments. As soil bulk density (g cm^{-3}) did not change from summer to winter, only the soil bulk density from the summer sampling is presented in the table.

	Sumer-Organic Matter (LOI %)	Winter-Organic Matter (LOI %)	Soil Bulk Density (g cm^{-3})	Soil Temperature (°C)
Flooded Site	9.8 (range: 6.8-14.0)	9.6 (range: 7.1-13.8)	0.93 (range: 0.83-1.13)	10.7 (range: 6.1-17.0)
Non-Flooded Site	25.4 (range: 21.1-28.2)	25.0 (range: 20.5-28.6)	0.57 (range: 0.52-0.65)	8.8 (range: 2.9-16.6)

3.2 CO2 Fluxes

Both the flooded and fallow winter management treatments resulted in a net flux of CO_2 to the atmosphere over the study period (10/31/12 – 3/5/13). The flooded-treatment site released a total of 21.05 g-C/m^2, while at the fallow-treatment site the total amount was slightly higher at 23.28 g-C/m^{-2}. Concomitant overall mean daily flux rates were similar; 1.7 g-C m^{-2}day^{-1} at the flooded-treatment site and 1.8 g-C m^{-2}day^{-1} at the fallow-treatment site. Mean daily rates of CO_2 emissions from these sites are at the upper end of the ranges reported by other studies from similar sites (**Table 4**). Daily flux values measured at the fallow-treatment site were surpassed by only one study, sited on a grazed, degraded peatland on Sherman Island, which is also in the Delta, just west of Staten Island (Baldocchi et al. 2010; Hatala et al. 2012). Emission rates for both sites are similar to those reported, for example, in freshwater marshes (Rocha and Goulden, 2008; Miller 2011), swamps (Bridgham and Richardson, 1992), and bogs (Lafleur et al. 2003). Flooding clearly had a large effect on emission rates. For example, the mean daily CO_2 flux was significantly greater at the flooded-treatment site for the period with no observed standing water (2.7 g-C m^{-2}day^{-1}) compared to when there was standing water (1.4 g-C m^{-2}day^{-1}; $p < 0.001$).

Despite the similarity in total annual emissions between treatments, large differences in daily emissions between treatments gave rise to periods exhibiting large disparities in concurrent daily emission rates, providing insights into underlying processes. Similar to other studies (Fang and Moncrief, 2001; Friborg et al. 1997; Kim et al. 1998; and many others), soil temperatures were found to have significant explanatory value for the daily rates of CO_2 emissions at both the fallow- and flooded-treatment sites. Soil moisture and, in the case of the flooded-treatment site, water table depth also had significant explanatory value for daily flux rates.

3.2.1 Temporal Variability

Despite similar soil temperature time series, there were distinct differences between treatments in the timing of maximum CO_2 emissions. During the flooded portion of the study period, the mean daily CO_2 emission rate for the flooded-treatment site was 1.4 g-C m^{-2}day^{-1}, which was significantly less than the fallow-treatment site (2.1 g-C m^{-2}day^{-1}; $p < 0.0001$), due largely to the strongly anaerobic conditions on the flooded-treatment site. Further, mean daily CO_2 emission rates for both sites were declining in apparent synchrony with air temperature in the early part of the record (**Figure 6**), they diverge with the onset of a series of rainfall events starting on 11/15/12, corresponding to a rise in soil temperature and a concomitant increase in aerobic soil respiration at the fallow-treatment site to a mean daily value of 3.5 g-C m^{-2}day^{-1} between 11/12/12-12/5/12. This period represents the time of greatest difference in CO_2 emission rates between the two sites ($p < 0.0001$). Soil temperatures also rose in the flooded-treatment site, but

mean daily CO_2 emission rates did not correspondingly increase during this period, but rather continued their previous decline to a mean daily value of 1.8 g-C $m^{-2}day^{-1}$ due to the strongly anaerobic conditions at the site. With additional rainfall and declining temperatures, the fallow-treatment site became saturated and emission rates at the two sites converged to a mean value of 0.9 g-C m^{-2} d^{-1} for the flooded-treatment site, and 1.0 g-C m^{-2} d^{-1} for the fallow-treatment site between 12/30/2012 and 2/1/2013.

Table 4: Summary of published winter carbon fluxes. Highest rates of CO_2 fluxes listed first, followed by CH_4 fluxes.

CO_2 Fluxes (g-C m^{-2} day^{-1})	CH_4 Fluxes (mg-C m^{-2} day^{-1})	Temperature (°C)	Conditions	Climate	Ecosystem	Method	Reference
~-3-8	52-415	~0-20[as]	Peat/Flooded	Mediterranean	Agriculture	EC	Baldocchi et al. 2011, Hatala et al. 2012, Y.A. Teh et al. 2011, Sonnentag et al. 2011
0.5-5.2	0.3-18.4	2.9-16.6[s]	Peat/Fallow	Mediterranean	Agriculture	EC	This study
~2-4.5**	N/A	~5-20[a]	Mineral/ Flooded>1m	Mediterranean	Freshwater Marsh	EC	Rocha and Goulden, 2008
~1.2-3.6	~0	~11[s]	Peat/Fallow/ Flooded	Mediterranean	Agriculture/ Wetland	Chambers	Miller 2011
0.4-3.5	-2.1-233.5	6.1-17.0[s]	Peat/Flooded	Mediterranean	Agriculture	EC	This study
0.2-1.7	26.9-114	N/A	Mineral/Flooded	Mediterranean	Agriculture	EC/Flux Gradient	McMillian et al. 2007
~1.2	N/A	N/A	Nutrient Deficient Peat*	Temperate-Humid	Pocosins/ Swamps	Alkali adsorption	Bridgham and Richardson, 1992
0.74-1.09	N/A	~1-(-4.5)[s]	Peat/Snow	Continental-cool	Bog	EC	Lafleur et al. 2003
~0.12-0.96	~0-0.1	0-4[s]	Peat (Dry-Wet)	Temperate	Bog-Forest-Heather	Chamber	Chapman and Thurlow, 1996
0.2-0.6	N/A	-9-1[m]	Mineral/Snow	Cool-temperate	Wetland	EC	Bonneville et al. 2008
~(-0.5)-0.6	N/A	~5-25[m]	Peat/Dry season	Tropical	Fresh water wetland	EC	Schedlbauer et al. 2010
0.065-0.59	N/A	N/A	Peat/Snow	Boreal	Mires	Chambers	Silvola et al. 1996
~0-0.55	N/A	N/A	Peat/Snow	Boreal-Subarctic	Temperate/ Bog/Fen	Modeled EC	Lindroth et al. 2007
0.31-0.52	0-30	~0[s]	Peat/Snow	Continental	Poor Fen	EC	Olson et al. 2013
N/A	~90-180	~5-7[s]	Peat/WTD<10cm	Temperate-Maritime	Grassland	Chambers	Hendriks et al. 2010
N/A	20-53	~-1-(-5.5)[a]	Peat/Flooded	Continental-humid	Poor Fen	Pore Water/ Chamber	Melloh and Crill, 1996
N/A	6.7 (estimated)	N/A	Litter/Mineral Soil	Humid-Continental	Marsh	EC	J. Kim et al. 1998
N/A	<3	4-10[s]	Peat-Mineral/ Flooded	Temperate-Maritime	Grassland/ Pasture	Chambers	Boeckx and Van Cleemput, 1997

[a]Air Temperature
[s]Daily mean soil temperature
[m]Monthly air temperature
*November and December
**Assumes Gross Ecosystem Exchange is zero, during senescent period.

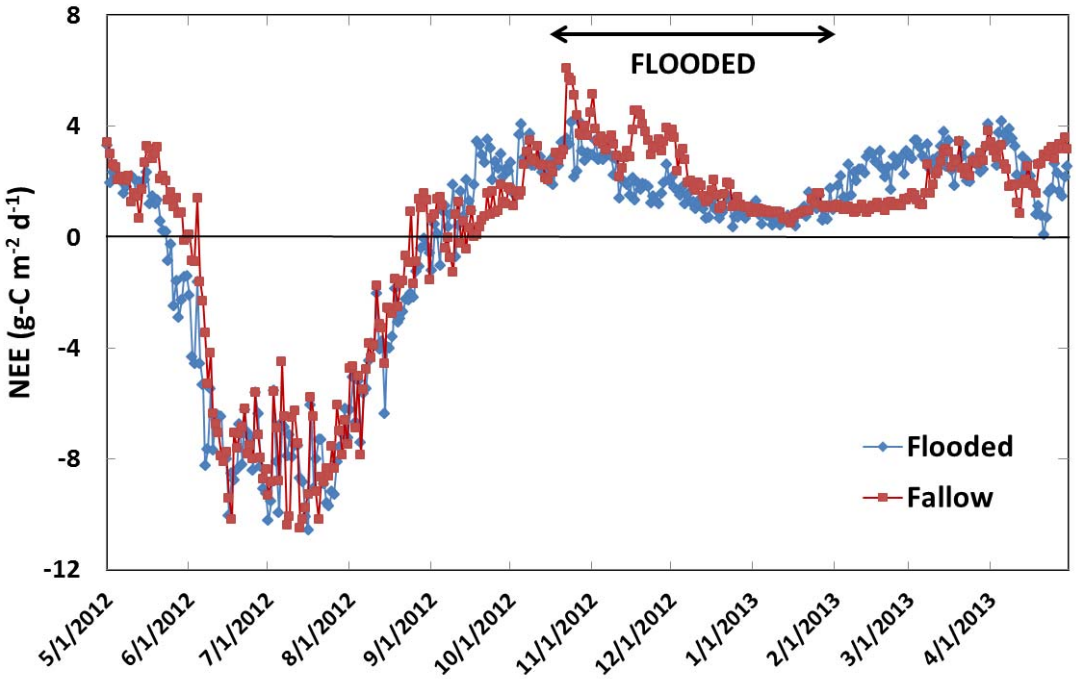

Figure 6: Net ecosystem exchange from both the flooded and non-flooded site.

Study period occurred between 10/31/12 through 3/5/13. The black arrows at the bottom of the graph represent the period of where water table depth (10/31/12-2/1/13) was recorded to be above the surface. Standing water was observed at the flooded site until 2/9/13.

Immediately following the time at which the flooded-treatment site was drained, a similar disparity in emission rates was observed, but this time with the flood-treatment site exhibiting higher rates. After the water table depth was below the surface at the flooded-treatment site (beginning February, 2013), the mean daily CO_2 flux at the flooded-treatment site increased to a maximum of 3.5 g-C $m^{-2}day^{-1}$ on 3/3/13 and was significantly greater than the mean CO_2 flux at the fallow-treatment site which remained relatively constant for this period (average 1.1 g-C $m^{-2}day^{-1}$; $p < 0.0001$). This disparity in emission rates persisted despite the similar rise in soil temperature in the two sites, and offset the greater emissions seen at the fallow-treatment site earlier in the season.

During the growing season (May through September), emission rates were almost identical for both sites (-481 and -464 g-C m^{-2} for the flooded and fallow treatment, respectively). Beyond the 2012/2013 annual measurements, fluxes were also measured at the flooded-treatment site for winter 2011/2012 (**Figure 10**) to permit assessment of inter-annual variability in flux and examination of process that may contribute to any observed difference. Air temperature and precipitation for November and December of 2011 were both below average (22percent and 64percent, respectively). Air temperatures rebounded in January and February of 2012 and were 5percent above average; however, precipitation was still below average (-33percent). For 2011, irrigation water was applied approximately 3 weeks later than in 2012. These conditions resulted in approximately a 21percent decrease in CO_2 emission. The results are consistent with the relationship between soil temperature and carbon fluxes observed in 2012/2013 and in many other studies (Lloyd and Taylor, 1994; Fredrig et al., 1997; Longdoz et al., 2000).

3.2.2 Drivers

The lower emissions rate at the fallow-treatment site during this period has a number of potential causes. The most significant is likely the growth of weeds at the fallow-treatment site beginning in February, which offset the effects of soil respiration. In contrast, the flooding treatment prevented weeds from establishing. At the fallow-treatment site, the CO_2 flux during the period with no weeds (2.0 g-C $m^{-2}day^{-1}$) was greater than the period when weeds were present (1.2 g-C $m^{-2}day^{-1}$; $p < 0.05$). Alternatively, it is also likely that the inventory of labile organic matter in the upper soil column was exhausted during the early period at the fallow treatment site, while remineralization of this material was delayed at the flooded-treatment site because of the anaerobic conditions. Once the water table lowered sufficiently at the flooded-treatment site, the labile organic material was subject to aerobic remineralization in an amount that balanced the early-season elevated flux from the fallow-treatment site. Soil isotopic data show a clear distinction between the $\delta^{13}C$ values of corn biomass (~ -14‰) and soils from various depths and sites (~-24 to -27‰), suggesting that the rapid aerobic mineralization of corn residue may drive the CO_2 pulse and limit the incorporation into soil organic matter (**Figure 7).**

Further evidence that the balance between aerobic and anaerobic respiration strongly affected the timing of elevated CO_2 flux is seen in the relationship between CO_2 fluxes and soil temperature for different periods within the record (**Figure 8**). At the flooded-treatment site, the slopes of the relationship were similar for the flooded versus drained period, but the fluxes were greatly suppressed when the field was flooded. At the fallow-treatment site, fluxes are much more responsive to temperature during the early period than the later period when weed growth offset soil respiration and when the inventory of labile organic material may have been exhausted. It is important to note that both anaerobic and aerobic respiration are sensitive to soil temperature. Other environmental variables, such as latent and sensible heat flux had significant explanatory value for daily CO_2 flux rates (r^2 ~ 0.36; **Table 5**), but these are not independent from soil temperature and moisture.

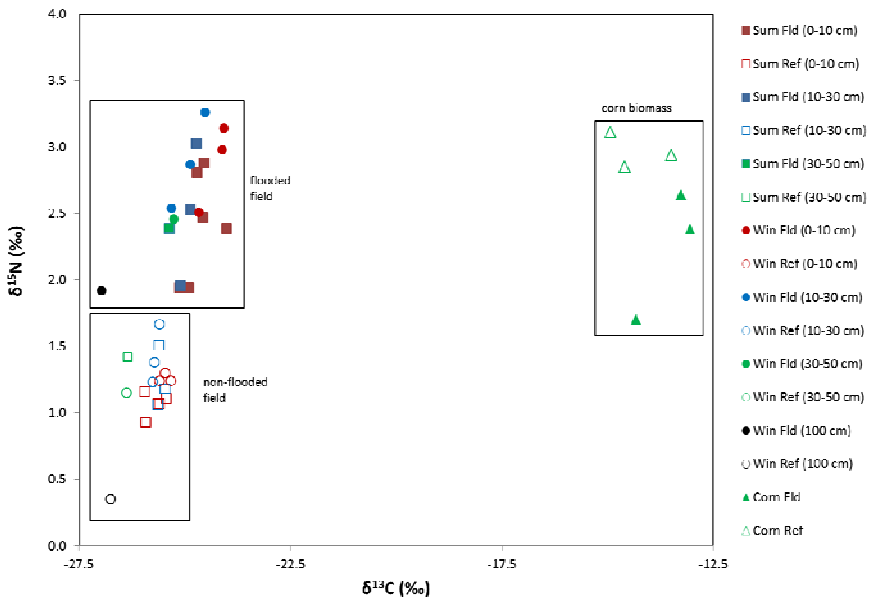

Figure 7: Soil isotopic values ($\delta^{13}C$ and $\delta^{15}N$, ‰) by site and depth, as well as isotopic values from corn biomass collected prior to harvest.

Results show a clear isotopic distinction between soils and corn.

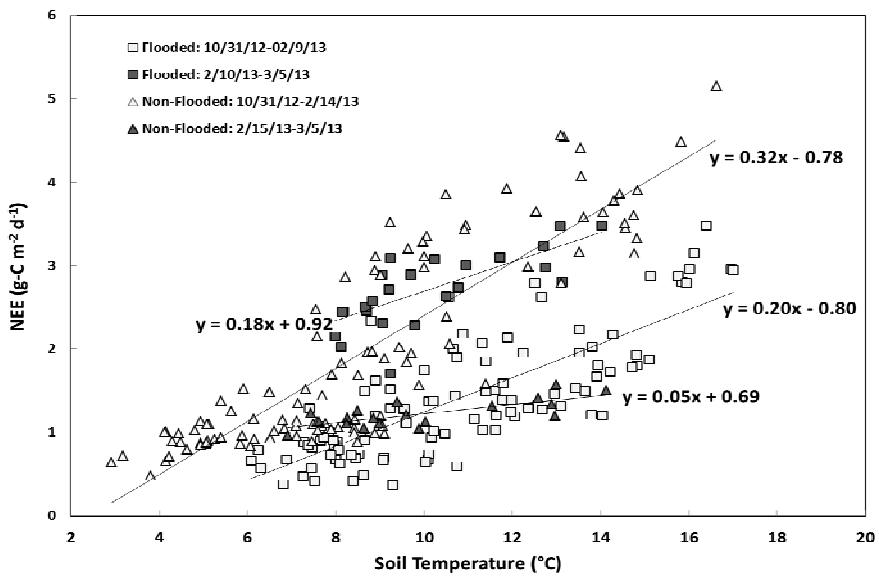

Figure 8: Regression analysis to determine the relationship between NEE and soil temperature under varying hydrological and field conditions.

Table 5: Regressions comparing CO_2 (g-C m^{-2} d^{-1}) fluxes measured at the flooded and non-flooded site with environmental variables, energy fluxes, and carbon fluxes.

Only variables with P < 0.05 are shown.

Treatment	*Indepen*dent Variable (*Var*)	CO_2 (g-C m^{-2} day^{-1}) Regression Equation	r^2	P
Flooded	Soil Temperature (°C)	$CO_2 = 0.18Var - 0.25$	0.31	<0.001
Flooded	Soil Moisture (m3 m^{-3})	$CO_2 = -48.9Var + 21.5$	0.26	<0.001
Flooded	Water Table Depth (m)	$CO_2 = -1.08Var + 1.8$	0.42	<0.001
Flooded	Pressure (kPa)	$CO_2 = -0.37Var + 40$	0.03	0.040
Flooded	Solar Radiation (MJ m^{-2} d^{-1})	$CO_2 = 0.09Var + 0.72$	0.22	<0.001
Flooded	Latent Heat Flux (MJ m^{-2} d^{-1})	$CO_2 = 0.52Var + 0.67$	0.37	<0.001
Flooded	Sensible Heat Flux (MJ m^{-2} d^{-1})	$CO_2 = 0.43Var + 1.33$	0.36	<0.001
Flooded	Ground Heat Flux (MJ m^{-2} d^{-1})	$CO_2 = -1.08Var + 1.95$	0.14	<0.001
Non-Flooded	Soil Temperature (°C)	$CO_2 = 0.28Var - 0.62$	0.61	<0.001
Non-Flooded	Soil Moisture (m3 m^{-3})	$CO_2 = -18.78Var + 11.50$	0.49	<0.001
Non-Flooded	Precipitation (mm)	$CO_2 = 1.74Var + 0.06$	0.08	0.001
Non-Flooded	Pressure (kPa)	$CO_2 = -1.06Var + 109.57$	0.15	<0.001
Non-Flooded	Solar Radiation (MJ m^{-2} d^{-1})	$CO_2 = -0.07Var + 2.67$	0.08	0.001
Non-Flooded	Latent Heat Flux (MJ m^{-2} d^{-1})	$CO_2 = 0.71Var + 0.89$	0.09	<0.001
Non-Flooded	Sensible Heat Flux (MJ m^{-2} d^{-1})	$CO_2 = -0.22Var + 2.24$	0.09	<0.001
Non-Flooded	Ground Heat Flux (MJ m^{-2} d^{-1})	$CO_2 = 0.46Var + 2.02$	0.04	0.027

3.3 CH4 Fluxes

Both fields were a net source of CH_4 emissions annually(**Figure 9**), but total carbon emitted as CH_4 was more than ten times higher at the flooded-treatment site (0.81 g C/m^{-2}) compared to the fallow-treatment site (0.07 g C/m^{-2}). Mean daily rates at the flooded-treatment site were 64.1 mg-C $m^{-2}day^{-1}$ and 5.9 mg-C $m^{-2}day^{-1}$ at the fallow-treatment site. As for the CO_2 emissions, annual CH_4 emissions from the flooded site were among the highest previously reported (**Table 4**), but were lower than the annual CH_4 emission rates measured at a pasture on Sherman Island in the western Delta (Baldocchi et al. 2010; Hatala et al. 2012). CH_4 fluxes measured in the study are

however within the ranges of those measured in peat grasslands (Hendriks et al. 2010), agricultural fields with peat soils (McMillian et al. 2007), and various types of wetlands (J. Kim et al. 1998; Melloh and Crill, 1996; Craft 2001). It is noteworthy that even the flux rates observed at the fallow-treatment site are similar to many freshwater wetlands (Bridgham et al., 2006). It is important to recognize that the highest CH_4 flux rates in this study were found in the winter, whereas for many sites, the highest anticipated fluxes are in the summer when soil temperatures are higher.

As for CO_2, the variation in the magnitude of the daily CH_4 flux over the duration of the study provides insights into underlying process and illuminates the different biogeochemistry of CH_4 and CO_2 emissions. Unlike CO_2 emissions, CH_4 emissions at the flooded-treatment site were more closely related to soil temperature and soil moisture than to water table depth. In contrast, for the fallow treatment, none of the measured environmental parameters had a significant relationship to CH_4 flux (**Table 6**).

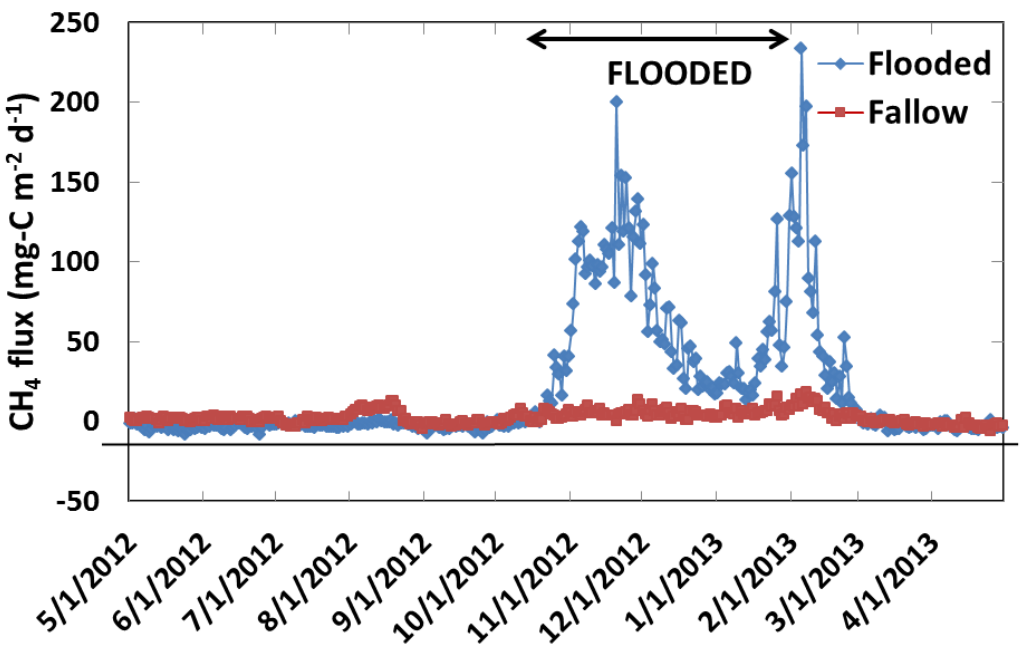

Figure 9: Daily mean CH_4 flux from both the flooded and non-flooded site.

Study period occurred between 10/31/12 through 3/5/13. The black arrows at the bottom of the graph represent the period of where water table depth (10/31/12-2/1/13) was recorded to be above the surface. Standing water was observed at the flooded site until 2/9/13.

Table 6: Regressions comparing CH_4 (g-C m^{-2} d^{-1}) fluxes measured at the flooded and non-flooded site with environmental variables, energy fluxes, and carbon fluxes.

Only variables with P < 0.05 are shown.

Treatment	*Indepen*dent Variable (*Var*)	CH_4 (g-C m^{-2} day^{-1}) Regression Equation	r^2	P
Flooded	Soil Temperature (°C)	$CH_4 = 8.58Var - 27.65$	0.23	<0.001
Flooded	Soil Moisture (m3 m^{-3})	$CH_4 = 2030.58Var - 758.35$	0.15	<0.001
Flooded	Pressure (kPa)	$CH_4 = -23.14Var + 2425.88$	0.04	0.019
Flooded	Sensible Heat Flux (MJ m^{-2} d^{-1})	$CH_4 = -10.27Var + 72.23$	0.07	0.003
Non-Flooded	Solar Radiation (MJ m^{-2} d^{-1})	$CH_4 = -1.48Var + 7.91$	0.04	0.025

3.3.1 Temporal Variability

There were marked differences in both the timing and the magnitude of the daily fluxes observed at the flooded and fallow treatments. The flooded-treatment site had two main periods of elevated CH_4 emissions (**see Figure 9**). The first period occurred in mid- to late-November, was characterized by a peak emission of approximately 200 mg-C $m^{-2}day^{-1}$ on 11/20/12 and was followed by several days with emission rates near 150 mg-C $m^{-2}day^{-1}$. The first peak emission occurred immediately following a rain event and the addition of irrigation water added to the field to increase overall water levels (11/13/12-11/19/12), which caused an increase in soil temperature. CH_4 emissions then progressively declined with soil temperature through mid-January, with daily mean rates were near 20 mg-C $m^{-2}day^{-1}$. CH_4 emission rates rose sharply in late January, coincident with draining of the field, with peak emission of 233.5 mg-C $m^{-2}day^{-1}$. This second period of elevated CH_4 emissions had a sharp peak period that lasted several days and occurred two to six days after water levels declined to below the land surface, suggesting induced biological activity caused these elevated emissions rather than release of hydrostatic pressure (see **Figure 10**). The increase in CH_4 emission rates coincided with the rapid elevation in CO_2 emissions, suggesting both were caused by rapidly increasing biological activity. Shortly afterward, CH_4 emissions declined sharply, compared to the first emission period, and rates were close to zero by March 1 as the field was prepared for planting.

At the fallow-treatment site, rates were comparatively low throughout the measurement period with numerous short-duration peaks through the record (**Figure 9**). Although CH_4 emission rates were roughly 10percent of the rates measured at the flooded-treatment site, there patterns of emission seemed to respond to similar processes. Once soils became saturated at the fallow-treatment site in late November, the daily mean CH_4 fluxes (Figure 4d) closely tracked soil temperatures. Emission rates began to rise near February 1 (Figure 4d), coincident with the rise in rates at the flooded-treatment site following drainage. As for the flooded-treatment, emission rates declined rapidly after mid-February. A simple linear regression analysis of CH_4 emissions

from both sites after 12/1/12 revealed that temporal variation at the sites were strongly related ($P<0.001$, $r^2 = 0.56$).

Comparison of the 2011/2012 CH_4 emissions to those of 2012/2013 suggested that the delaying flood up of the flooded-treatment field by three weeks resulted in a 53percent reduction in CH_4 emission. This was largely a consequence of lower soil temperatures at flood up which mitigated the early-season peak in emissions seen in the 2012/2013 record.

3.3.2 Drivers

For the study as a whole, CH_4 emissions were found to have a significant ($P<0.001$) relationship with soil temperature and soil moisture, but the explanatory power was quite poor ($r^2=0.15$ and $r^2=0.23$, respectively; **Table 6**). However, for the period when the field was flooded, there was a stronger relationship between emissions and soil temperature ($P<0.001$; $r^2 = 0.51$) and emissions and water table depth ($P<0.001$; $r^2 = 0.40$).

To examine the relative importance of underlying drivers, mean daily CH_4 fluxes at the flooded-treatment site were separated into four periods by methane emission level; (1) declining emissions from 10/31/12-1/4/13, (2) elevated emissions from 1/5/13-2/1/13, (3) elevated emissions during field drainage from 2/1/13-2/9/13, and (4) declining emissions during the drying period from 2/10/13-3/5/13 (**Figure 10, Table 7**). Emission rates were found to be strongly related to soil temperature for the first two inundated periods ($P<0.001$; $r^2 = 0.46$ and 0.64, respectively) and the drying period ($P<0.005$, $r^2=0.32$), while no significant relationship was found for the drainage period ($P>0.05$; $r^2=0.07$). Water table depth was more strongly related to CH_4 emission once the field was dry ($P<0.001$, $r^2=0.68$).

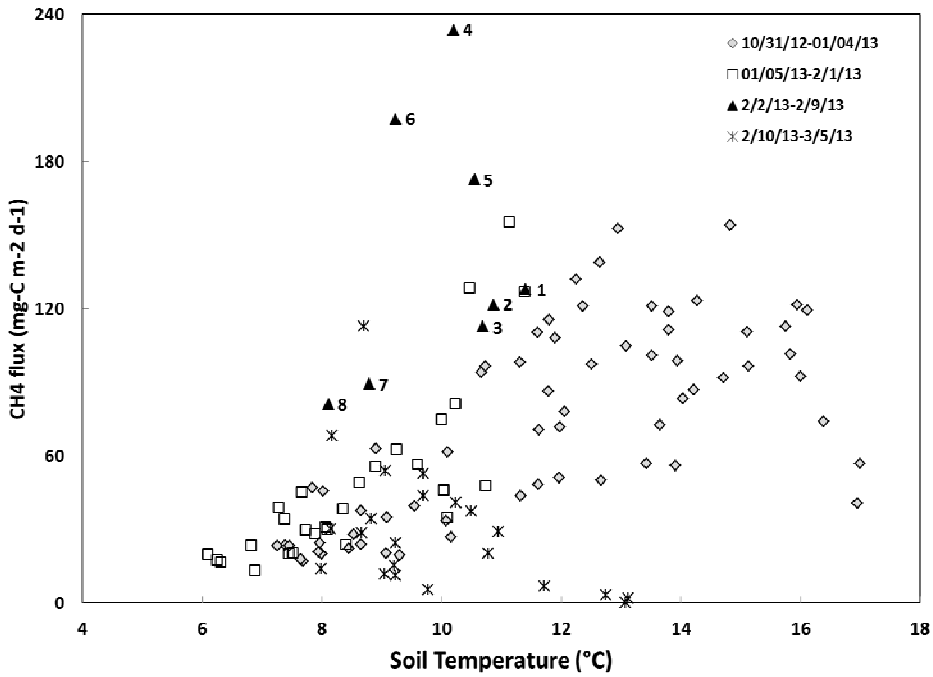

Figure 10*:* Mean daily CH_4 fluxes plotted together with mean daily soil temperatures

To determine relationships when there are changes in CH_4 emissions (peaks 1 and 2) and field conditions (flooded, initial drain period, and fallow).

Table 7: CH_4 versus mean daily soil temperatures for varying hydrological and field conditions.

Standard deviations are given in parenthesis for CH_4 and soil temperatures.

Field Observations	Period	Mean CH_4 (mg-C m^{-2} day^{-1})	Mean Soil Temperature (°C)	Slope Intercept	r^2	P
Peak 1	10/31/12-1/4/13	74.9 (41.9)	11.9 (2.8)	$CH_4 = 10.1Ts - 44.9$	0.46	<0.001
Peak 2 (no drain)	1/5/13-2/1/13	48.3 (36.0)	8.5 (1.5)	$CH_4 = 18.6Ts + 110.6$	0.64	<0.001
Drain	2/2/13-2/9/13	142.0 (53.9)	10.0 (1.2)	$CH_4 = 12.4Ts + 17.7$	0.07	>0.05
Fallow (drying)	2/10/13-3/5/13	26.8 (26.6)	10.2 (1.8)	$CH_4 = -8.4Ts + 113.0$	0.32	<0.005

CHAPTER 4: Discussion

High winter CO_2 fluxes were measured at both the flooded and non-flooded-treatment sites, as were elevated CH_4 fluxes, with the measured CH_4 flux at the flooded-treatment site an order of magnitude greater than the non-flooded-treatment site, and high in comparison to other published studies from similar environments. These findings highlight the importance of including wintertime measurements in estimating annual budgets. In terms of gaseous carbon balance, both systems were essentially carbon neutral. The flooded-treatment site was a slight carbon sink (~-39 g-C m^{-2} y^{-1}) and the non-flooded-treatment site was a slight carbon source (~47 g-C m^{-2} y^{-1}), but when the removal of carbon from the system due to grain harvest is considered (~530 g-C m^{-2} y^{-1}; Brent Tadman, land manager, personal communication; Hernandez-Ramirez et al., 2011), both systems are net sources of carbon. If the export of dissolved carbon through the hydrologic system from the flooded-treatment site were quantified, flooding would have clearly resulted in a greater loss of carbon than the non-flooded treatment. Given that these flux rates are quite high and comparable to rates reported in the literature for wetlands, it seems likely that conversion of these sites to wetlands will not result in significant changes to the net carbon balance. This may be important in areas where wetland restoration is contemplated for the purpose of improving aquatic or avian habitat.

The flooding of peat soils was found to reduce CO_2 fluxes during the flooded period, consistent with the management goal of reducing oxidative loss of soil organic material. However, this effect was largely confined to the periods of flooding. As discussed above, the annual carbon balance was approximately equal between sites, with the flooded-treatment site having lower fluxes during the flooded period and higher fluxes during the non-flooded period, particularly during the transitional period from flooding. Contributing to this effect is the successful suppression of weed growth by flood treatment – one of the management goals. Weed growth at the fallow-treatment site offset the CO_2 efflux due to soil respiration.

This study found that although there was significantly more CH_4 released from the flooded-treatment site, the net global warming potential of the flooded treatment was similar to that of the fallow treatment if the grain harvest and the gas fluxes are combined. Expressed in CO_2-equivalent mass units, the flooded-treatment site emits 21.5 MT CO_{2e} $ha^{-1}yr^{-1}$, while the fallow-treatment site emits 21.2 MT CO_{2e} $ha^{-1}yr^{-1}$. The flooded treatment site also must account for the carbon present in the drained flood waters, which can be estimated to elevate the total emissions for the flood treatment site to 25 MT CO_{2e} $ha^{-1}yr^{-1}$. If the methane source was eliminated or reduced, the treatments would be similar. Methane flux represents ~2percent of the gaseous carbon leaving the flooded-treatment site, while it represents only ~0.1percent at the non-flooded-treatment site.

Another important finding was that soil temperature was correlated with both CH_4 and CO_2 fluxes at both sites, while other environmental variables such as energy balance, solar radiation, wind speed, and soil moisture were more variably or weakly correlated. Precipitation was also not strongly correlated to measured fluxes, likely due to the highly managed hydrology at these sites. Soil temperature was best correlated with CH_4 fluxes during the flooded period in the flood treatment (r^2=0.46-0.64; **Table 7**), and best correlated with CO_2 fluxes at the non-flooded-treatment site (r^2=0.61; **Table 5**).

These findings have important implications for fluxes under future climate conditions. For example, the higher night time temperatures projected for the region (Cayan et al., 2009) may cause a non-linear increase in soil temperature, and will therefore likely result in fluxes elevated above those observed in this study for both CH_4 and CO_2. The implication is that soil oxidation rates and CO_2 fluxes will likely increase in the future under both treatments. Elevated CH_4 fluxes from winter-flooded fields further exacerbate this effect and greatly elevate the global warming potential (GWP), particularly under warming conditions. Given that flooding did not reduce oxidative loss of peat soils, policy makers will need to balance the relative benefits of flooding for wildlife habitat against that of increased GWP caused by the treatment.

While intentional flooding did increase CH_4 emissions, the results also suggest that CH_4 emissions from the flooded treatment might be lowered by alternative hydrologic management strategies. For example, adjusting the timing and duration of flooding may reduce emissions as suggested when comparing CH_4 emissions across the two winter seasons. During the second winter, all harvest activities were concluded by the end of September and the field was flooded almost three weeks earlier than the previous year (late October), during which harvest was delayed by three to four weeks due to cool air temperatures and cloudy conditions. The most important difference between the two years was the lack of a peak CH_4 emission period in November and December of 2011 (**Figure 11**). This first peak emission period in 2012 made up 63percent of the total CH_4 emission period for the entire 2012/2013 winter season and based on the results from 2011, is most likely due to warmer conditions during flood up. The mean daily CH_4 fluxes - the GWP of which were greater than for CO_2 in both years - were sensitive to the early flooding and resulted in winter totals for 2012/2013 that were 91percent higher than those of winter 2011/2012. This suggests that delaying flooding until soil temperatures decrease may be one relatively simple management action that could reduce the amount of CH_4 emitted by nearly half.

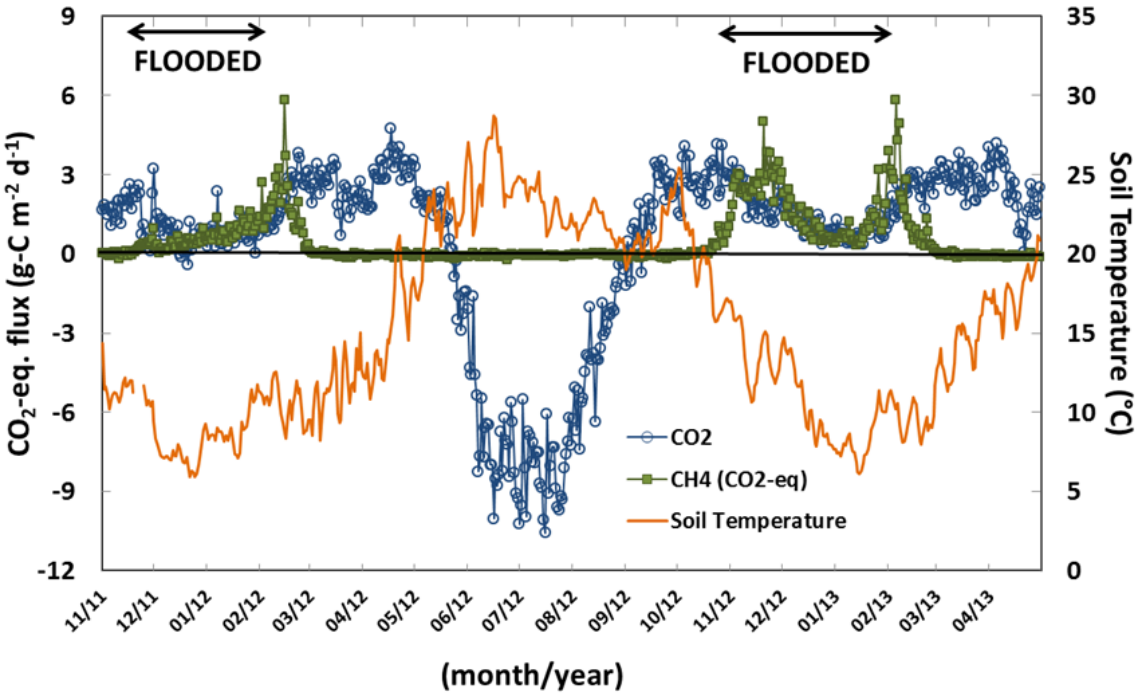

Figure 11: Mean daily CO_2 and CO_2-equivalent CH_4 fluxes compared against the mean daily soil temperature at the flooded site.

The first flooded period (November 2011 through January 2012) was approximately three weeks shorter than the second flooded period (October 2012 through January 2013). Mean soil temperatures were below 10°C at the onset of the first flooded season and above 15°C when the second flooded period began.

CHAPTER 5: Conclusions

This study investigated the CO_2 and CH_4 emission rates from agricultural operations on peat soils. Baseline data was obtained and comparisons were made for two common soil management techniques: leaving the field fallow in the winter and flooding the field in winter. Winter flooding is intended to reduce the oxidative loss of soil organic matter, reduce erosion, improve soil texture, provide habitat for water fowl, as well as other putative benefits. The concern is that while winter flooding may lower overall carbon loss from the field, it may lead to higher production of CH_4, with a concomitant increase in the global warming potential of the total emissions.

Both treatments had high annual rates of CO_2 flux as well as elevated CH_4 fluxes. Mean annual rates of CH_4 flux at the flooded-treatment site were an order of magnitude greater than the non-flooded-treatment site, and among the highest reported in the literature, indicating this management technique significantly increases the GWP of field emissions over the fallow treatment. Further, mean annual rates of CO_2 flux indicate that winter flooding does not suppress oxidation of the peat soils. Total carbon loss rates from the flooded treatment are estimated to be higher than the fallow treatment when grain harvest and loss of carbon through the hydrologic system are factored in. The results of this study highlight the importance of understanding how Delta agricultural land and water management can effect GHG emissions.

We suggest that answering the following questions may help further clarify the drivers and management strategies appropriate for reducing GHG from winter flooded agricultural lands in the Delta:

1) **What is the relative importance of corn residue versus peat as a labile source of organic matter for GHG production?** *There is evidence in this study that the labile organic material in the crop residue left on the field may preferentially lead to CH_4 production either directly or because it induces CH_4 production in the native peat organic material, but the data in this study is inconclusive.*
2) **Can the timing of intentional flooding alter the magnitude of GHG fluxes?** *While the data suggest that the timing of flooding is critical, future efforts should test the hypothesis that flooding during colder conditions could reduce CH_4 emissions by as much as half.*
3) **How do the measured GHG emissions compare more broadly to other crop types and water management scenarios in the Delta?** *Given the need to better understand baseline GHG emissions across the Delta, future detailed studies comparing sites with different land uses, crop types, cropping practices and irrigation are warranted.*
4) **How do changes in water management affect nitrous oxide (N_2O) dynamics on corn fields?** *A limitation in the study was the lack of a nitrous oxide analyzer for continuous measurements on the eddy flux towers. Similarly, problems with chamber measurements inthe*

study precluded a clear interpretation of effects of winter flooding on N_2O. Future studies that quantify N_2O flux before, during and after winter flooding will be useful for a full evaluation of impacts on GHG emissions.

Information obtained from these broader and more detailed studies can inform land managers about baseline conditions and management strategies that reduce GHG emissions from Delta agricultural peatlands. The information in turn can be used to create an incentive structure that supports reductions in GHG emissions while providing other environmental benefits such as winter waterfowl habitat.

REFERENCES

Aubinet, M., T. Vesala, and D. Papale, (2012), Eddy Covariance: A Practical Guide to Measurement and Data Analysis, Springer, Dordrecht, Netherlands.

Baldocchi, D., and E. Waller, (2012), Analysis of the Relationship between Fog, Winter Chill Accumulation and Solar Energy in the Center Valley. California Energy Commission. Publication Number: CEC-500-2010-035

Baldocchi, D., M. Detto, O. Sonnentag, J. Verfaillie, Y. Teh, W. Silver, and N. Kelly, (2012), The challenges of measuring methane fluxes and concentrations over a peatland pasture, Agr. Forest Meteorolology, 153: 177–187.

Bellisario, L. M., J. L. Bubier, T. R. Moore, and J. Chanton, (1999), Controls on CH4 emissions from a northern peatland, Global Biogeochemical Cycles, 13: 81–92.

Bouwman, A. F., L. J. M. Boumans, and N. H. Batjes, (2002), Modeling global annual N2O and NO emissions from fertilized fields, Global Biogeochemical Cycles, 16(4): 1080. doi:10.1029/2001GB001812.

Brigham, S.D., J.P. Megonigal, J.K. Keller, N.P. Bliss, and C. Trettin, (2006), The carbon balance of North American wetlands. Wetlands, 26:889-916.

Bridgham, S. D., and C. J. Richardson, (1992) Mechanisms controlling soil respiration (CO2 and CH4) in southern peatlands. Soil Biology and Biochemistry, 24:1089–1099.

Bubier, J. L., G. Bhatia, T. R. Moore, N. T. Roulet, and P. M. Lafleur, (2003), Between year and site variability in growing season net ecosystem CO2 exchange at a large peatland, Ontario, Canada, Ecosystems, 6: 353-367.

Cayan, D., M. Tyree, M. Dettinger, H. Hidalgo, T. Das, E. Maurer, P. Bromirski, N. Graham, and R. Flick., (2009), Climate change scenarios and sea level rise estimates for the California 2008 Climate Change Scenarios Assessment. California Energy Commission Final Report (CEC-500-2009-014-D).

Central Valley Joint Venture, (2006), Central Valley Joint Venture Implementation Plan—conserving bird habitat. U.S. Fish and Wildlife Service, Sacramento, California, USA. http://www.centralvalleyjointventure.org/assets/pdf/CVJV_fnl.pdf (last accessed on 9/28/13)

Chanton J.P., G.J. Whiting, J.D. Happell, and G. Gerard, (1993), Contrasting rates and diurnal patterns of methane emission from emergent aquatic macrophytes, Aquatic Botany, 46: 111–128.

Cloern J.E., N. Knowles, L.R. Brown, D. Cayan, M.D. Dettinger et al., (2011), Projected Evolution of California's San Francisco Bay-Delta-River System in a Century of Climate Change. PLoS ONE 6(9): e24465. doi:10.1371/journal.pone.0024465.

Craft, C.B., (2001), Biology of wetland soils, in Wetland Soils, Richardson, J.L. and Vepraskas, M.J., Eds., Lewis Publishers, Boca Raton, FL., p. 107-135.

De Gryze, S., A. Wolf, S.R. Kaffka, J. Mitchell, D.E. Rolston, S.R. Temple, J. Lee, and J. Six (2010) Simulating greenhouse gas budgets of four California cropping systems under conventional and alternative management. Ecological Applications 20:1805–1819.

Denmead, O.T., (1991), Sources and sinks of greenhouse gases in the soil-plant environment. Vegetation, 91: 73-86.

Deverel, S.J. and S. Rojstaczer, (1996), Subsidence of agricultural lands in the Sacramento-San Joaquin Delta, California: Role of aqueous and gaseous carbon fluxes. Water Resources Research, 32(8): 2359-2367.

Deverel, S.J. and D.A. Leighton, (2010), Historic, Recent, and Future Subsidence, Sacramento-San Joaquin Delta, California, USA. San Francisco Estuary and Watershed Science, 8: 1-23.

Dettinger, M., (2013), Atmospheric rivers as Drought Busters on the U.S. West Coast. Journal of Hydrometeorology, . doi:10.1175/JHM-D-13-02.1.

Drexler, J.Z., C.S. de Fontaine, and T.A. Brown, (2009a), Peat accretion histories during the past 6,000 years in the marshes of the Sacramento-San Joaquin Delta, CA, USA, Estuaries and Coasts, 32: 871-892.

Drexler, J.Z., C.S. de Fontaine, and S.J. Deverel, (2009b), The legacy of wetland drainage on the remaining peat in the Sacramento-San Joaquin Delta, California, USA. Wetlands, 29: 372-386.

Fang, C. and J.B. Moncrieff, (2001), The dependence of soil CO2 efflux on temperature. Soil Biology and Biochemistry, 33: 155–165.

Friborg, T., T. R. Christensen, and H. Søgaard, (1997), Rapid response of greenhouse gas emission to early spring thaw in a subarctic mire as shown by micrometeorological techniques, Geophysical Research Letters, 24(22): 3061–3066.

Hatala, J. A., M. Detto, O. Sonnentag, S.J. Deverel, J. Verfaillie, and D.D. Baldocchi, (2012), Greenhouse gas (CO2, CH4, H2O) fluxes from drained and flooded agricultural peatlands in the Sacramento-San Joaquin Delta. Agriculture Ecosystems and Environment, 150: 1-18.

Hendriks D.M.D, J. van Huissteden, and A.J. Dolman, (2010), Multi-technique assessment of spatial and temporal variability of methane fluxes in a peat meadow. Agricultural and Forest Meteorology, 150: 757–774.

Hernandez-Ramirez, G., J.L. Hatfield, T.B. Parkin, T.J. Sauer, and J.H. Prueger, (2011), Carbon dioxide fluxes in corn-soybean rotation in the midwestern U.S.: Inter- and intra-annual variations, and biophysical controls. Agricultural and Forest Meteorology 151(12): 1831-1842, doi:http://dx.doi.org/10.1016/j.agrformet.2011.07.017

Ivey, GL, CP Herziger, and M. Gause, (2003), Farming for wildlife: an overview of agricultural operations at Staten Island, San Joaquin County, California. Galt, CA: The Nature Conservancy. http://www.conawayranch.com/files/u1/FINALSTATENISLAND-FarmingforWildlife_stc.pdf (last accessed Sept. 28, 2013)

Juszczak, R., Humphreys, E., Acosta, M., Michalak-Galczewska, M., Kayzer, D., and J. Olejnik, (2013), Ecosystem respiration in a heterogeneous temperate peatland and its sensitivity to peat temperature and water table depth. Plant and Soil, 366(1-2): 505-520.

Kasimir-Klemedtsson A, L Klemedtsson, K Berglund, P Martikainen, J Silvola and O Oenema, (1997), Greenhouse gas emissions from farmed organic soils: a review. Soil Use and Management, 13: 245-250.

Kim J., S.B. Verma, and D.P. Billesbach, (1998), Seasonal variation in methane emission from a temperate Phragmites-dominated marsh: effect of growth stage and plant-mediated transport. Global Change Biology, 5: 433–440.

Lai DYF, NT Roulet, ER Humphreys, TR Moore, and M. Dalva, (2012), The effect of atmospheric turbulence and chamber deployment period on autochamber CO2 and CH4 flux measurements in an ombrotrophic peatland. Biogeosciences Discussions, 9: 439–1482.

Lafleur, P. M., N. T. Roulet, J. L. Bubier, S. Frolking, and T. R. Moore, (2003), Interannual variability in the peatland-atmosphere carbon dioxide exchange at an ombrotrophic bog, Global Biogeochemical Cycles, 17, 1036, doi:10.1029/2002GB001983, 2.

Li, C., S. Frolking, X. Xiao, B. Moore III, S. Boles, J. Qiu, Y. Huang, W. Salas, and R. Sass, (2005), Modeling impacts of farming management alternatives on CO2, CH4, and N2O emissions: A case study for water management of rice agriculture of China, Global Biogeochemical Cycles, 19, GB3010, doi:10.1029/2004GB002341.

Lindroth, A., Lund, M., Nilsson, M., Aurela, M., Christensen, T. R., Laurila, T., Rinne, J., Riutta, T., Sagerfors, J., Strom, L., Tuovinen, J.-P. and Vesala, T., (2007), Environmental controls on the CO2 exchange in north European mires. Tellus B, 59: 812–825.

Lloyd J and JA Taylor, (1994), On the temperature dependence of soil respiration. Functional Ecology, 8: 315-323.

Longdoz B, M Yernaux, and M Aubinet, (2000), Soil CO2 efflux measurements in a mixed forest: impact of chamber disturbances, spatial variability and seasonal evolution. Global Change Biology, 6: 907-917.

McMillan A.M.S, M.L. Goulden, S.C. Tyler, (2007), Stoichiometry of CH4 and CO2 flux in a California rice paddy. Journal of Geophysical Research, 112: G01008.

Melloh, R. A., and P. M. Crill, (1996), Winter methane dynamics in a temperate peatland, Global Biogeochemical Cycles, 10(2): 247–254.

Miller, R., (2011), Carbon Gas Fluxes in Re-Established Wetlands on Organic Soils Differ Relative to Plant Community and Hydrology. Wetlands, 31(6): 1055-1066.

Miller, R.L., M. Fram, R. Fujii, and G. Wheeler, (2008), Subsidence reversal in a re-established wetland in the Sacramento-San Joaquin Delta, California, USA. San Francisco Estuary and Watershed Science, 6(3): 1-20.

Paustian K., C.V. Cole, D. Sauerbeck and N. Sampson, (1998), CO2 mitigation by agriculture: An overview. Climate Change, 40(1): 135-162.

Pogson, T.H. and S.M. Lindstedt, (1991), Distribution and abundance of large sandhill cranes, Grus Canadensis, wintering in California's Central Valley. The Condor, 93: 266-278.

Miyata A., R. Leuning, O.T. Denmead, J. Kim, Y. Harazono, (2000), Carbon dioxide and methane fluxes from an intermittently flooded paddy field. Agricultural and Forest Meteorology, 102: 287–303.

Moffat, A. M., D. Papale, M. Reichstein, D.Y. Hollinger, A.D. Richardson, A.G. Barr, and V.J. Stauch, (2007), Comprehensive comparison of gap-filling techniques for eddy covariance net carbon fluxes. Agricultural and Forest Meteorology, 147(3–4): 209-232.

Moore, T. R. and M. Dalva, (1993), The influence of temperature and water table position on carbon dioxide and methane emissions from laboratory columns of peatland soils. Journal of Soil Science, 44: 651–664.

Reichstein, M., E. Falge, D. Baldocchi, D. Papale, M. Aubinet, P. Berbigier, and R. Valentini. (2005). On the separation of net ecosystem exchange into assimilation and ecosystem respiration: review and improved algorithm. Global Change Biology, 11(9): 1424-1439.

Rocha, A. V., and M. L. Goulden, (2008), Large interannual CO2 and energy exchange variability in a freshwater marsh under consistent environmental conditions, Journal of Geophysical Research, 113, G04019, doi:10.1029/2008JG000712.

Schotanus, P., F.T.M. Nieuwstadt, and H.A.R. Bruin, (1983), Temperature measurement with a sonic anemometer and its application to heat and moisture fluxes. Boundary-Layer Meteorology, 26(1), 81-93. doi: 10.1007/bf00164332.

Topp, E. and Pattey, E, (1997), Soils as sources and sinks for atmospheric methane. Canadian Journal of Soil Science, 77: 167-178.

Webb, E. K., G.I. Pearman and R. Leuning, (1980), Correction of flux measurements for density effects due to heat and water vapour transfer. Quarterly Journal of the Royal Meteorological Society, 106(447): 85-100.

APPENDIX A:

Soil Chemical Properties

Appendix Table 1. Soil chemical properties from the flooded and non-flooded field at Staten Island. Samples were collected during the summer (2012) and winter (2013) to evaluate changes due to flooding. Methods for soil collection are described in section 2.8. Samples were collected from several depth intervals at six sites per field. Only a subset of sample locations and depths were analyzed during both periods.

Site & Soil Depth	Summer 2012 (Before Flooding)								Winter 2013 (After Flooding)							
	Bulk Density (g/vol)	pH	% Nitrogen	% Carbon	C:N	NH4-N	NO3-N	% OM (LOI)	Bulk Density (g/vol)	pH	% Nitrogen	% Carbon	C:N	NH4-N	NO3-N	% OM (LOI)
Flooded 1: 0 -10 cm	0.83	5.56	0.57	8.06	14.24	9.17	9.67	14.00	0.78	5.48	0.59	8.25	14.03	8.22	39.30	13.82
Flooded 1: 10 - 30 cm	0.91	5.64	0.56	7.83	13.93	6.72	12.47	13.46	0.87	5.59	0.56	7.80	13.93	6.77	19.10	13.24
Flooded 2: 0 -10 cm	0.82	5.50	0.37	5.37	14.44	5.27	14.72	9.34								
Flooded 2: 10 - 30 cm	1.18	5.67	0.35	4.95	14.06	4.52	5.42	8.70								
Flooded 3: 0 -10 cm	0.95	5.62	0.29	4.06	14.00	3.73	8.52	7.13	0.88	5.29	0.31	4.30	13.96	5.02	33.80	7.35
Flooded 3: 10 - 30 cm	1.13	5.64	0.28	3.89	13.75	3.09	1.72	6.82	1.06	5.43	0.30	4.11	13.75	4.66	15.80	7.08
Flooded 4: 0 -10 cm	0.90	5.56	0.31	4.43	14.24	4.10	17.62	7.76								
Flooded 4: 10 - 30 cm	1.14	5.61	0.30	4.14	14.03	3.20	4.65	7.27								
Flooded 5: 0 -10 cm	0.86	5.63	0.37	5.13	13.98	3.82	13.77	8.63	0.96	5.37	0.37	5.15	13.96	5.82	32.30	8.20
Flooded 5: 10 - 30 cm	0.88	5.53	0.36	4.92	13.86	4.19	7.82	8.67	1.18	5.59	0.36	4.99	13.82	3.63	12.40	7.88
Flooded 5: 30 - 50 cm			0.31	4.57	14.93			8.02			0.33	4.68	14.40			8.09
Flooded 5: 100 cm											0.65	9.83	15.08			17.10
Flooded 6: 0 -10 cm	0.65	5.66	0.67	9.31	14.00	8.57	16.07	15.56								
Flooded 6: 10 - 30 cm	0.82	5.72	0.66	9.24	14.02	6.57	4.72	13.94								
Flooded Mean	0.92	5.61	0.41	5.84	14.11	5.25	9.76	9.95	0.96	5.46	0.43	6.14	14.12	5.69	25.45	10.35
Non-Flooded 1: 0 -10 cm	0.65	6.36	1.21	16.60	13.73	11.52	10.32	26.49	0.51	6.47	1.17	16.60	14.25	8.02	18.30	27.37
Non-Flooded 1: 10 - 30 cm	0.54	6.33	1.23	16.67	13.52	8.67	24.12	24.05	0.59	6.60	1.16	16.34	14.15	7.27	20.90	20.50
Non-Flooded 2: 0 -10 cm	0.54	6.20	1.21	16.66	13.77	7.57	31.07	27.79								
Non-Flooded 2: 10 - 30 cm	0.50	6.63	1.17	16.53	14.10	7.72	9.27	24.13								
Non-Flooded 3: 0 -10 cm	0.58	6.42	1.25	17.31	13.88	7.57	7.07	28.25	0.53	6.45	1.20	17.45	14.54	8.67	16.50	28.56
Non-Flooded 3: 10 - 30 cm	0.52	6.70	1.17	16.95	14.50	8.37	8.02	24.22	0.63	6.45	1.19	17.03	14.34	7.17	12.80	23.84
Non-Flooded 4: 0 -10 cm	0.56	6.33	1.20	17.34	14.40	9.52	17.42	27.81								
Non-Flooded 4: 10 - 30 cm	0.56	6.73	1.20	17.10	14.25	7.92	12.37	23.71								
Non-Flooded 5: 0 -10 cm	0.53	6.40	1.19	17.01	14.26	9.07	10.02	28.07	0.60	6.77	1.22	17.33	14.16	7.72	12.00	22.71
Non-Flooded 5: 10 - 30 cm	0.59	6.69	1.24	16.72	13.52	7.82	5.22	21.10	0.57	6.67	1.21	17.03	14.06	6.67	13.70	27.14
Non-Flooded 5: 30 - 50 cm			1.20	17.79	14.85			29.31			1.33	19.96	14.97			31.90
Non-Flooded 5: 100 cm											0.74	11.83	15.92			19.23
Non-Flooded 6: 0 -10 cm	0.52	6.26	1.20	16.93	14.13	7.67	8.42	28.58								
Non-Flooded 6: 10 - 30 cm	0.57	6.62	1.20	16.95	14.08	8.22	6.62	28.39								
Non-Flooded Mean	0.56	6.47	1.21	16.97	14.08	8.47	12.50	26.30	0.57	6.57	1.15	16.70	14.55	7.59	15.70	25.16

Soil Isotopic Data

Appendix Table 2. Soil isotopic data ($\delta^{13}C$ and $\delta^{15}N$) from the flooded and non-flooded fields at Staten Island during summer (2012) and winter (2013). Samples were collected from two depths (0-10 cm, and 10-30 cm) as described in section 2.8. Samples were also composited for a 0-30 cm integrated value. Each value is the average of approximately six samples.

Site & Soil Depth	Summer 2012 (Before Flooding)		Winter 2013 (After Flooding)	
	d13C	d15N	d13C	d15N
Flooded Mean (0 - 10 cm)	-24.68	2.43	-24.29	2.88
Flooded Stdev (0 - 10 cm)	0.21	0.47	0.33	0.33
Flooded Mean (10 - 30 cm)	-24.91	2.51	-24.91	2.89
Flooded Stdev (10 - 30 cm)	0.19	0.54	0.40	0.36
Flooded Mean (0 - 30 cm)	-24.80	2.47	-24.60	2.88
Flooded Stdev (0 - 30 cm)	0.22	0.45	0.47	0.31
Non-Flooded Mean (0 - 10 cm)	-25.66	1.11	-25.47	1.26
Non-Flooded Stdev (0 - 10 cm)	0.26	0.05	0.13	0.03
Non-Flooded Mean (10 - 30 cm)	-25.58	1.25	-25.69	1.43
Non-Flooded Stdev (10 - 30 cm)	0.09	0.23	0.08	0.22
Non-Flooded Mean (0 - 30 cm)	-25.62	1.18	-25.58	1.34
Non-Flooded Stdev (0 - 30 cm)	0.18	0.17	0.16	0.17

Daily Eddy Flux and Meteorological Data

Data available upon request.